

Electromagnetic inverse problems in biomedical engineering

Jens Haueisen

Institute of Biomedical Engineering and Informatics, Technical University of Ilmenau,
Germany

Biomagnetic Center, Department of Neurology, University Jena, Germany

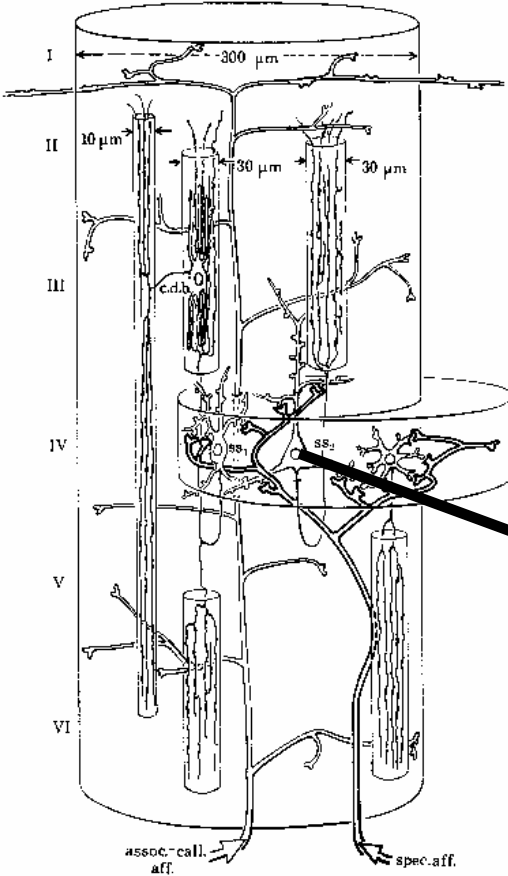
Overview

1. Introduction
2. Localization of magnetic markers in the alimentary tract
3. The influence of forward model conductivities on EEG/MEG source reconstruction
4. Optimization of magnetic sensor arrays for magnetocardiography
5. Validation of source reconstruction procedures

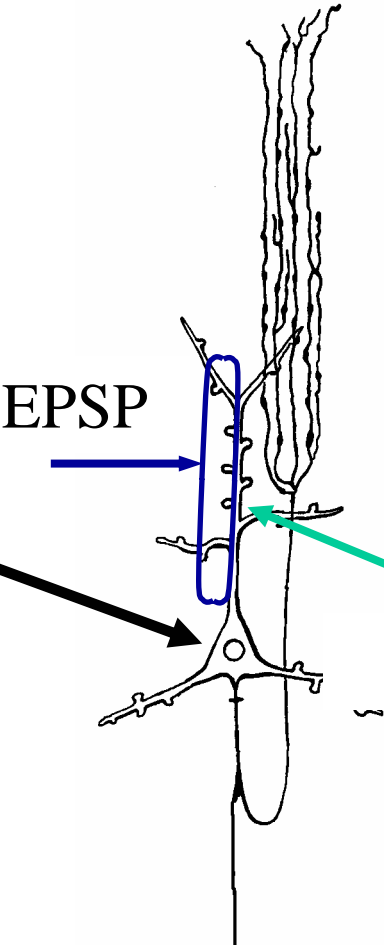
Introduction

Genesis of bioelectromagnetic fields and potentials

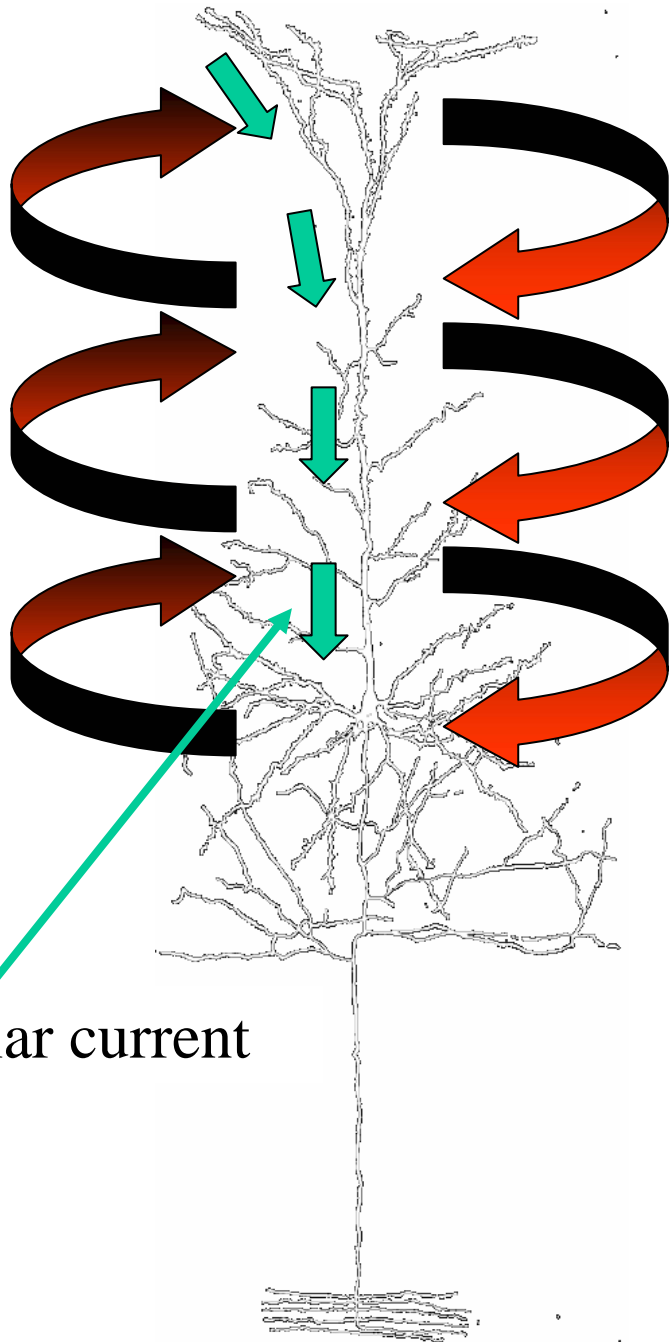
Cortical column

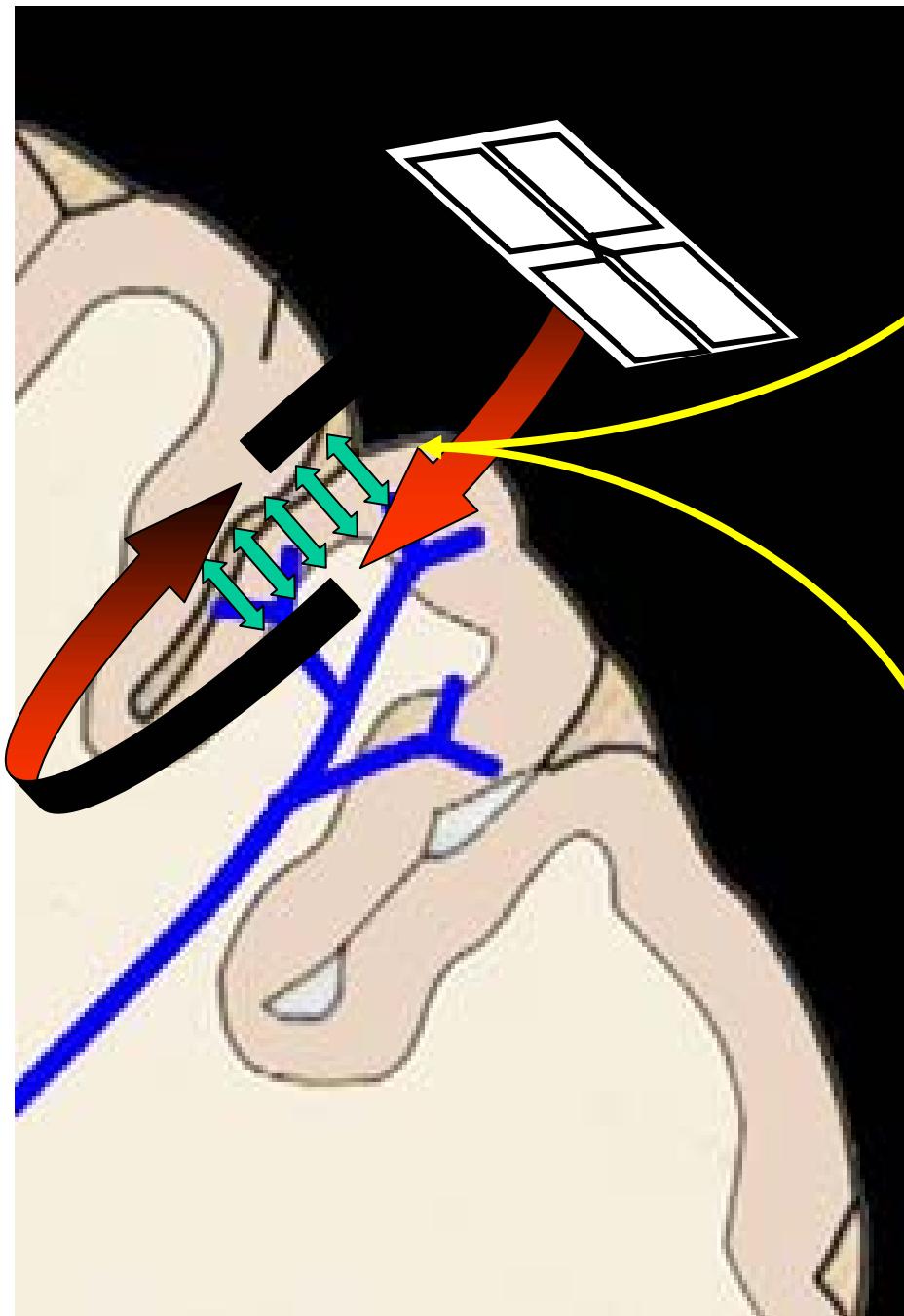


Pyramidal cell



intracellular current

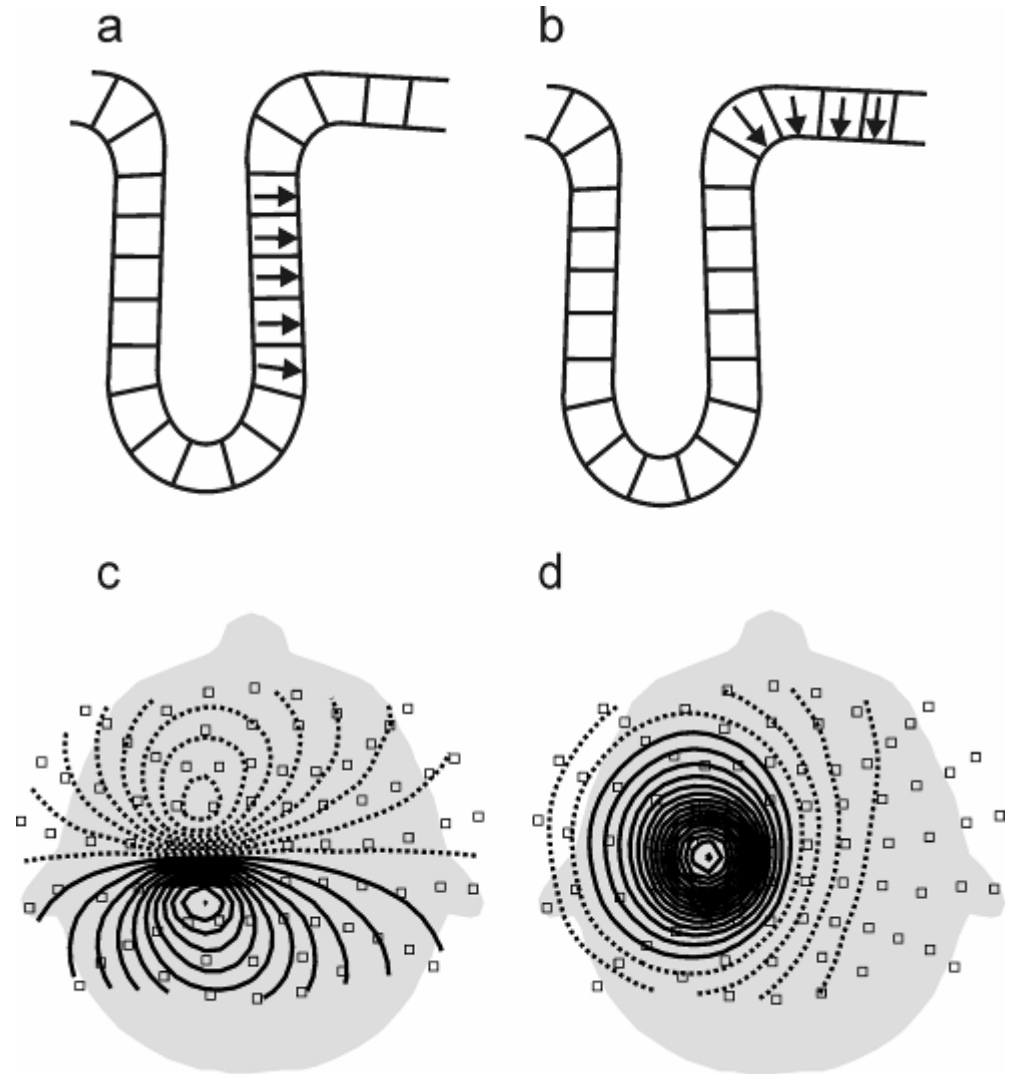




Genesis of bioelectromagnetic fields and potentials

(a) and (c): tangential direction

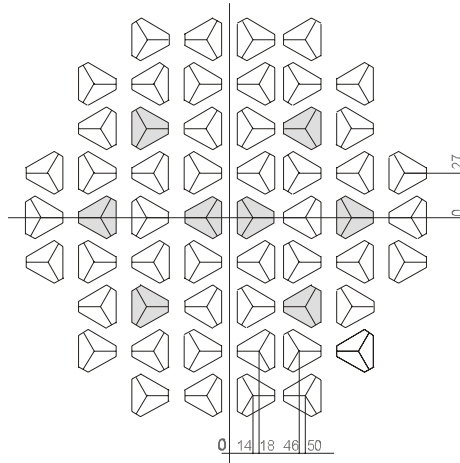
(b) and (d): radial direction



Measurement of biomagnetic fields

Argos 200

ATB (Chieti, Italy)



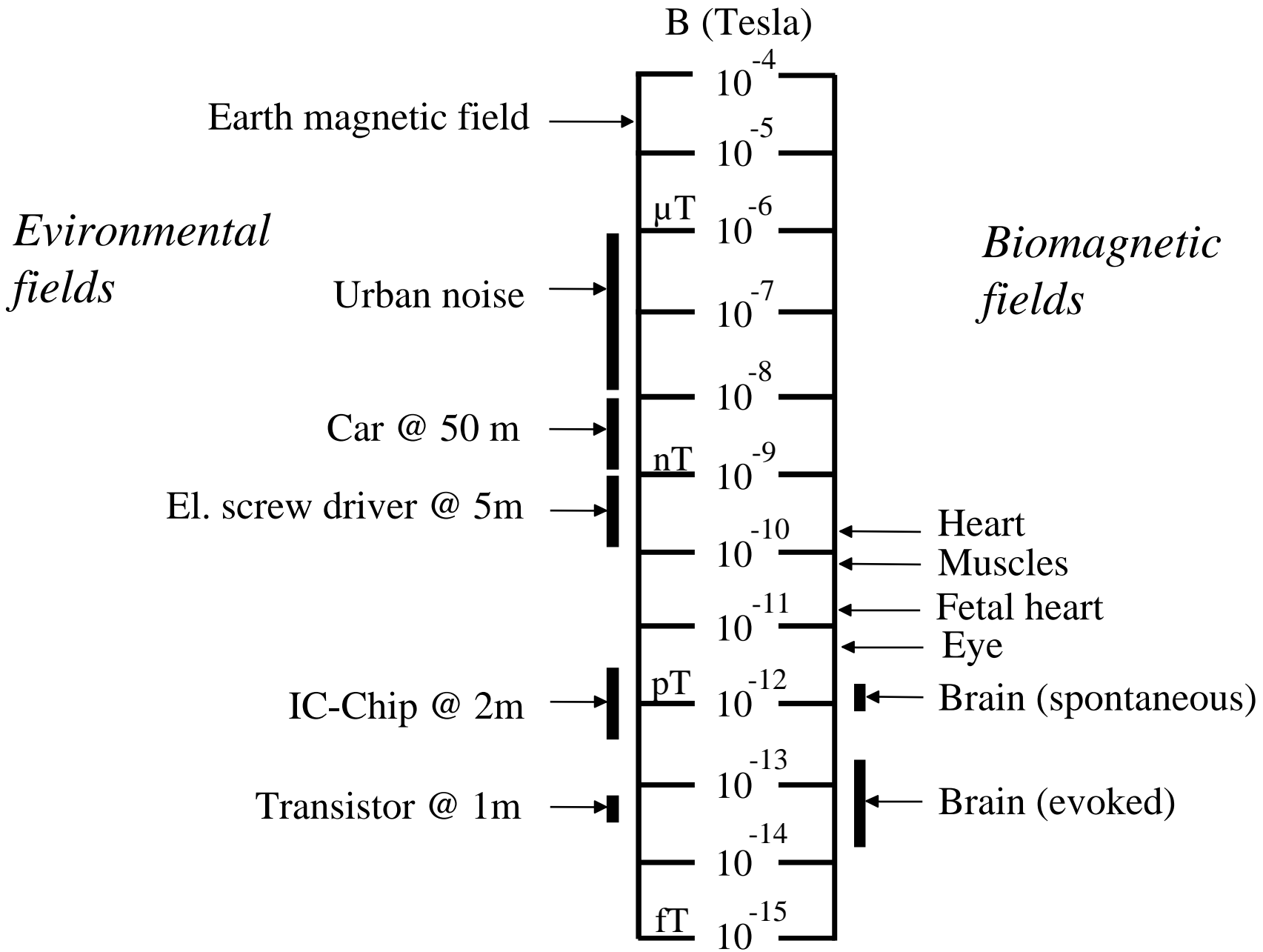
Vectorview

Neuromag

(Helsinki, Finland)

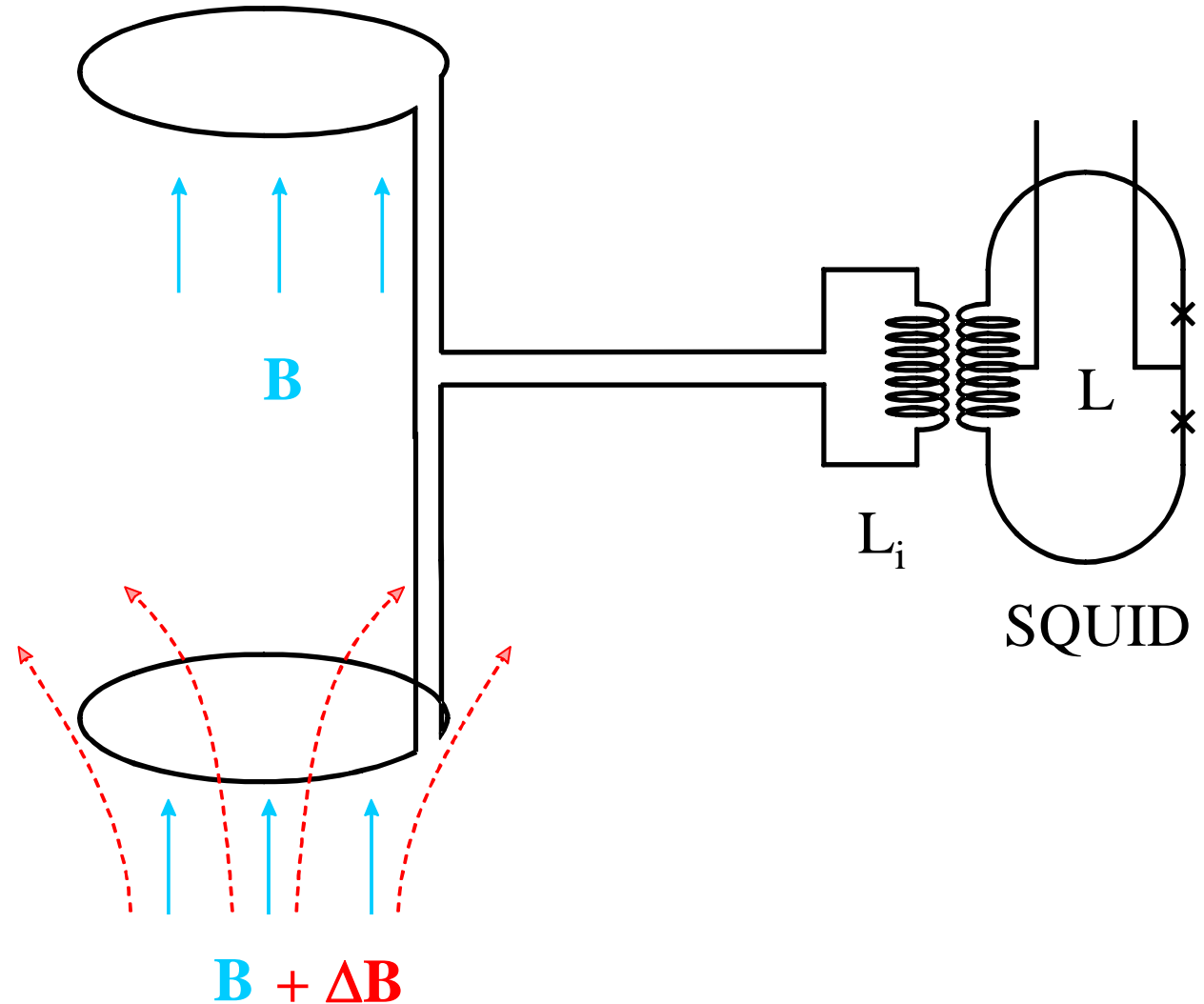


Comparison of typical amplitudes of the magnetic induction B



Magnetometer and Gradiometer

Reference coil



Pick up coil

$B + \Delta B$

Magnetic shielding

Goal:

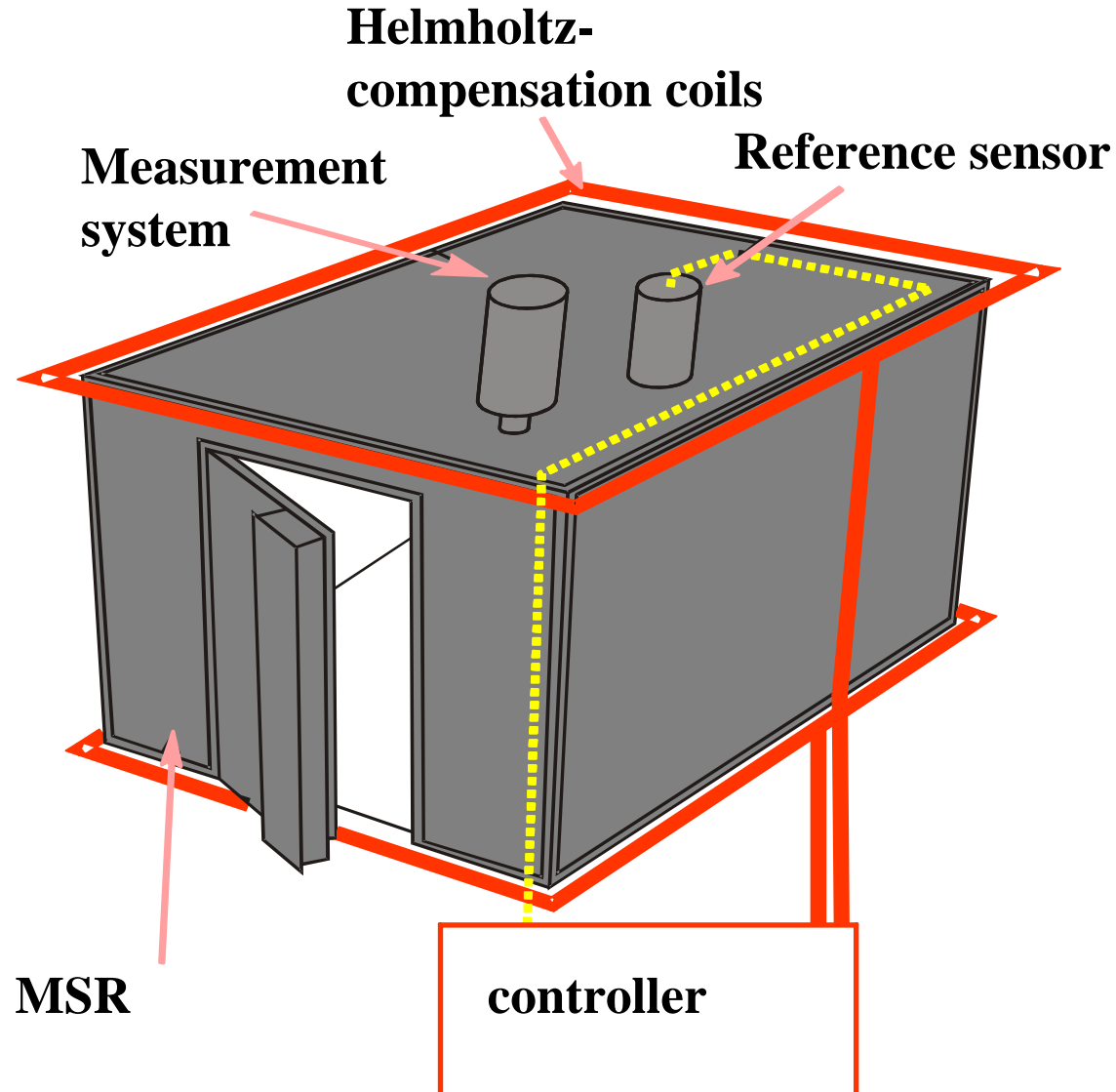
Shielding against external disturbances

Design criteria:

Compromise between costs and shielding

Realization:

Passive
Active

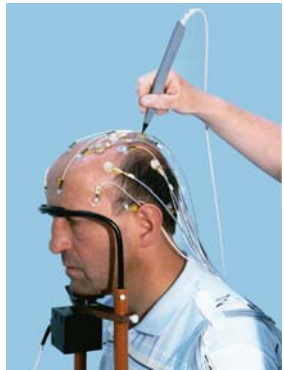


Source reconstruction overview

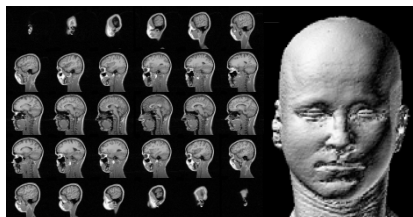
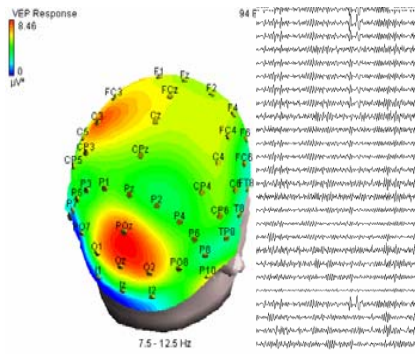
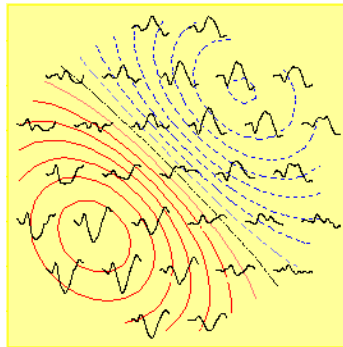


Institut für Biomedizinische
Technik und Informatik

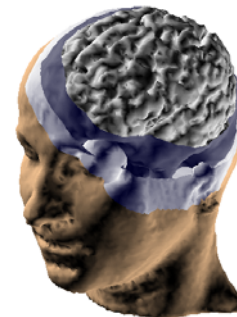
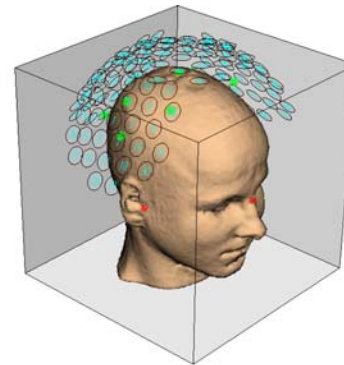
Measurements



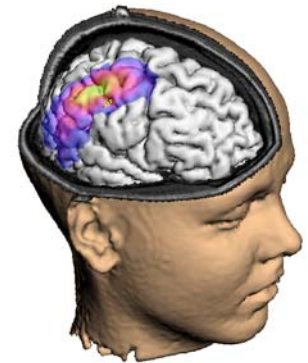
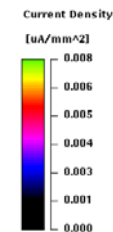
Data



Models



Results and Interpretation



Solution of the inverse problem

Problem

Measurement data

Forward problem

Inverse problem

Sources



Overview

1. Introduction
2. Localization of magnetic markers in the alimentary tract
 1. Multipole method
 2. Simulations
 3. Phantom measurements
 4. Clinical study
3. The influence of forward model conductivities on EEG/MEG source reconstruction
4. Optimization of magnetic sensor arrays for magnetocardiography
5. Validation of source reconstruction procedures

Localization of magnetic markers in the alimentary tract

- **Motivation:**
 - **Analysis of tract motion (peristalsis)**
 - **Passage / throughput times**
 - **targeted disposal of drugs**
- **Methods:**
 - **Magnetically marked capsules**
 - **Fast and robust method for (online) localization**
- **Problem:**
 - **Interferences**
- **Solution:**
 - **Multipole approach for simultaneous localization and external noise compensation**

State of the art

- **Noise suppression with various methods**
- **Marker localization with non-linear search methods (Simplex, Levenberg-Marquardt, Gauss-Newton)**

Multipole method

- **Multipole expansion of the measured magnetic field with inner and outer components (multipoles)**
- **Comparison of coefficients of the Taylor series expansion of the magnetic dipole field with inner multipoles yields a system of equations for the determination of the dipole location and moment from the inner multipole of 1st and 2nd order**
- **Noise cancelation by elimination of outer components**
- **Iterative usage in time series analysis**

Inner components

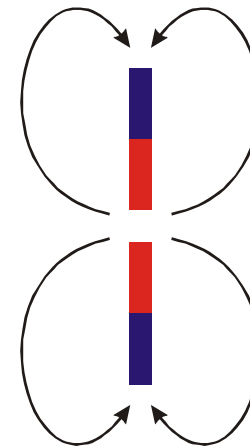
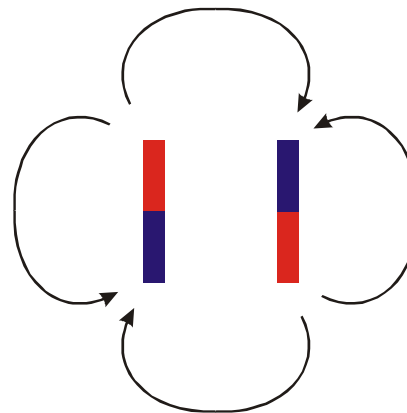
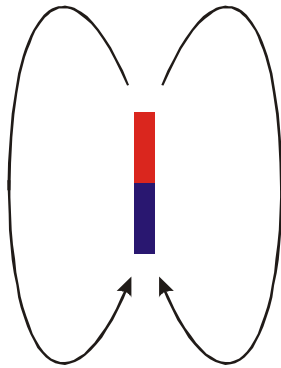
Dipole
First order tensor

Quadrupole
Second order tensor

symmetric

3 linearly independent
components

5 linearly independent
components



Outer components

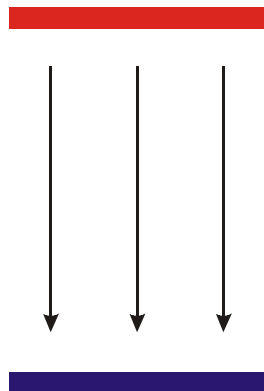
First order tensor

Second order tensor

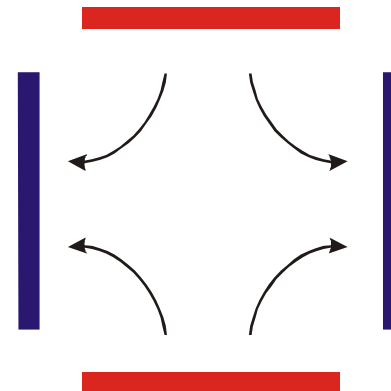
symmetric

3 linearly independent
components

5 linearly independent
components



homogeneous
disturbing
field
of 0th order

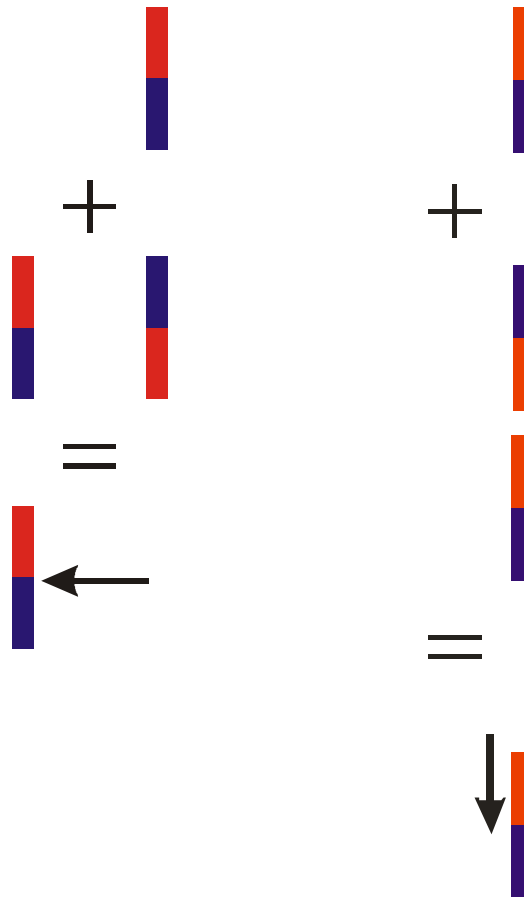


gradient
disturbing
field
of 1st order

Localization and noise separation

Inner components

location and place of
the marker are
reconstructed from
the dipole und
quadrupole at
coordinate center



Separation of outer components as noise.

Multipole expansion

Multipole expansion for the field of a magnetic marker close to (0,0,0):

$$\begin{aligned} \vec{B}_m(\vec{r}) = & \frac{\mu_0}{4\pi} \sum_{j=1}^3 \left(F_m^{i,j}(\vec{r}) \right)_{i=1}^3 c_j^m + \frac{\mu_0}{4\pi} \sum_{k=1}^3 \sum_{j=1}^3 \left(F_m^{i,j,k}(\vec{r}) \right)_{i=1}^3 c_{j,k}^m \\ & + \frac{\mu_0}{4\pi} \sum_{l=1}^3 \sum_{k=1}^3 \sum_{j=1}^3 \left(F_m^{i,j,k,l}(\vec{r}) \right)_{i=1}^3 c_{j,k,l}^m + \dots \end{aligned}$$

Form functions F can be treated as Taylor series expansion:

$$\begin{aligned} F_m^i &= \frac{x_i}{r^3}, & F_m^{i,j} &= -\frac{\partial F_m^j}{\partial x_i}, \\ F_m^{i,j,k} &= -\frac{\partial F_m^{j,k}}{\partial x_i}, & F_m^{i,j,k,l} &= -\frac{\partial F_m^{j,k,l}}{\partial x_i}. \end{aligned}$$

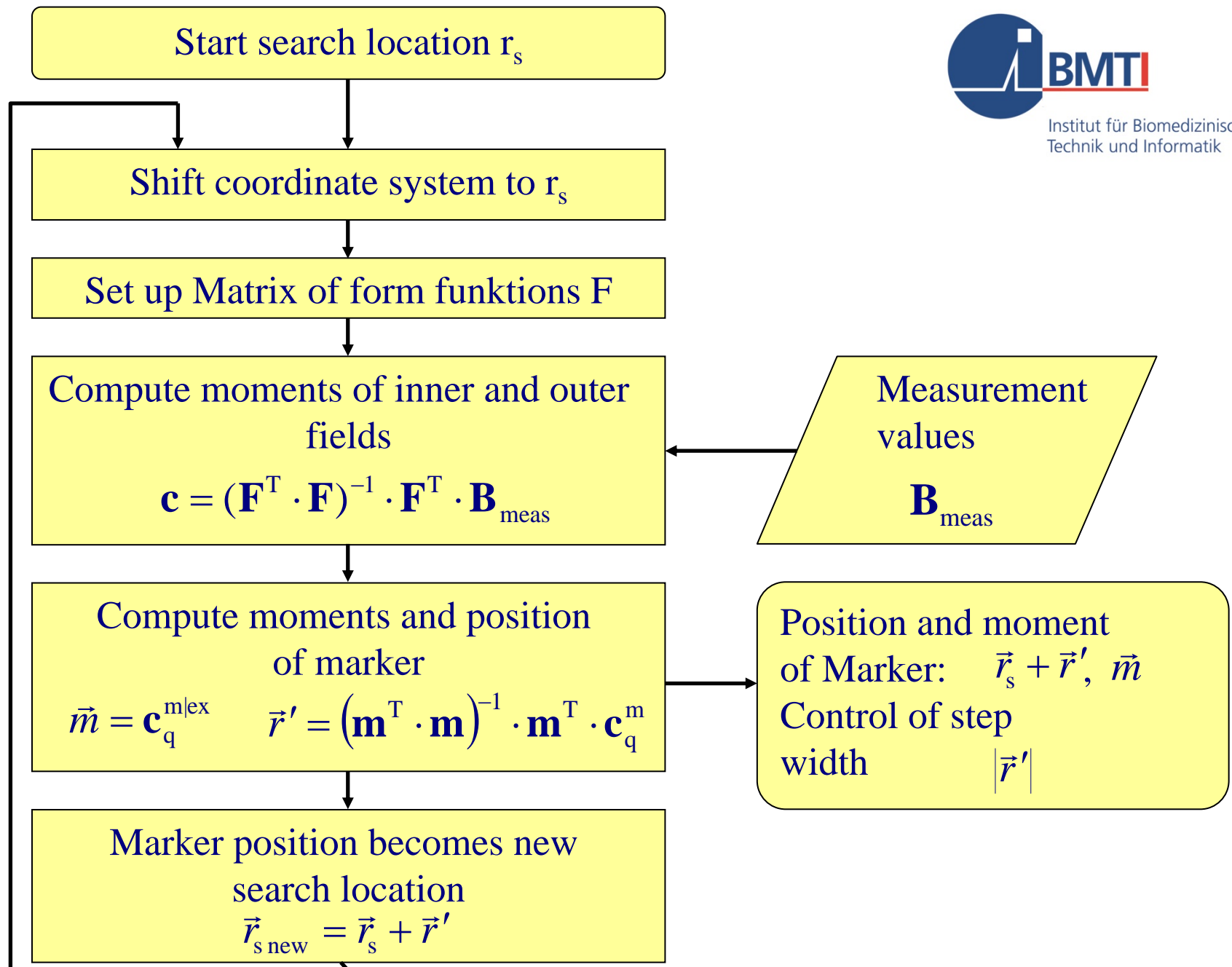
Multipole expansion

Multipole expansion for the field of distant external noise sources:

$$\begin{aligned}\vec{B}_{\text{ex}}(\vec{r}) = & \frac{\mu_0}{4\pi} \sum_{j=1}^3 \left(F_{\text{ex}}^{i,j}(\vec{r}) \right)_{i=1}^3 c_j^{\text{ex}} + \frac{\mu_0}{4\pi} \sum_{k=1}^3 \sum_{j=1}^3 \left(F_{\text{ex}}^{i,j,k}(\vec{r}) \right)_{i=1}^3 c_{j,k}^{\text{ex}} \\ & + \frac{\mu_0}{4\pi} \sum_{l=1}^3 \sum_{k=1}^3 \sum_{j=1}^3 \left(F_{\text{ex}}^{i,j,k,l}(\vec{r}) \right)_{i=1}^3 c_{j,k,l}^{\text{ex}} + \dots\end{aligned}$$

Form functions for external sources derived from the inner sources:

$$F_{\text{ex}}^{i,j} = \frac{\partial(F_m^j r^3)}{\partial x_i}, \quad F_{\text{ex}}^{i,j,k} = \frac{\partial(F_m^{j,k} r^5)}{\partial x_i}, \quad F_{\text{ex}}^{i,j,k,l} = \frac{\partial(F_m^{j,k,l} r^7)}{\partial x_i}$$



Simulation setup

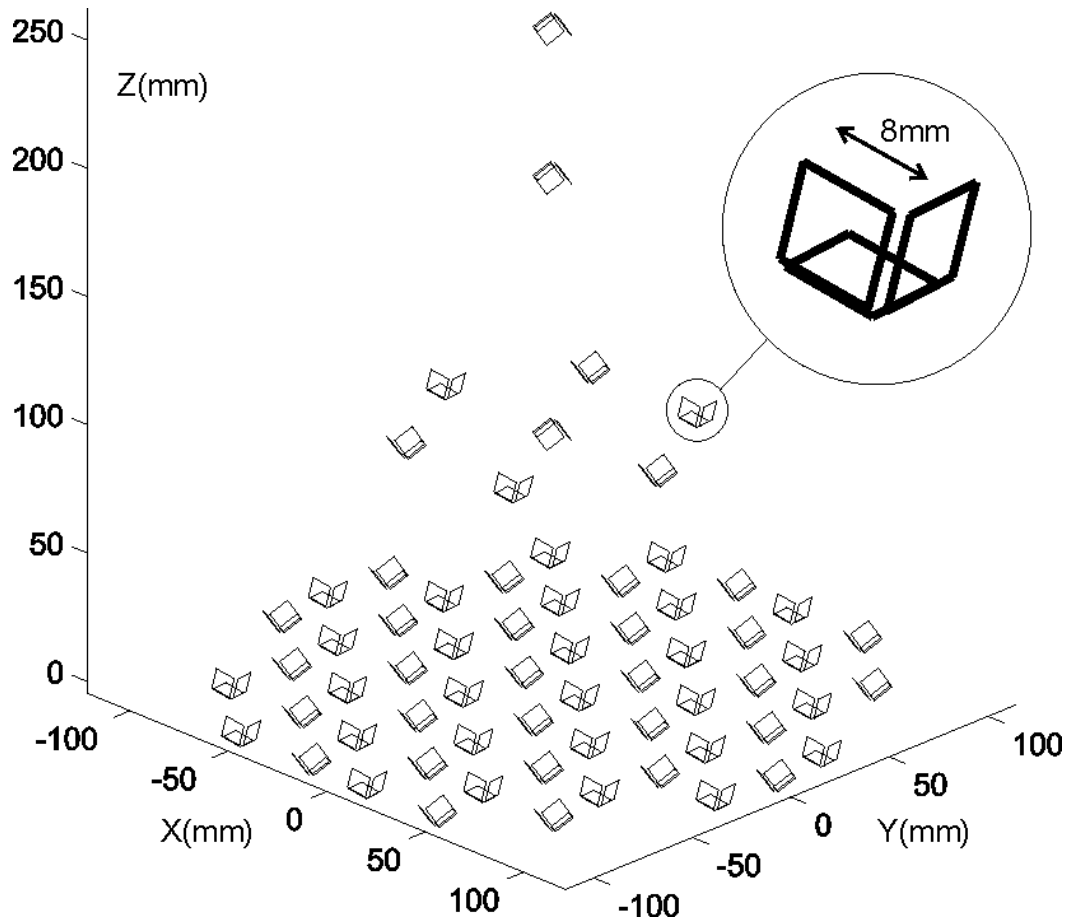
Aims:

- Localization error as a function of noise
- Localization error after one step, as function of starting distance
- Convergence distance depending on noise level

Set up:

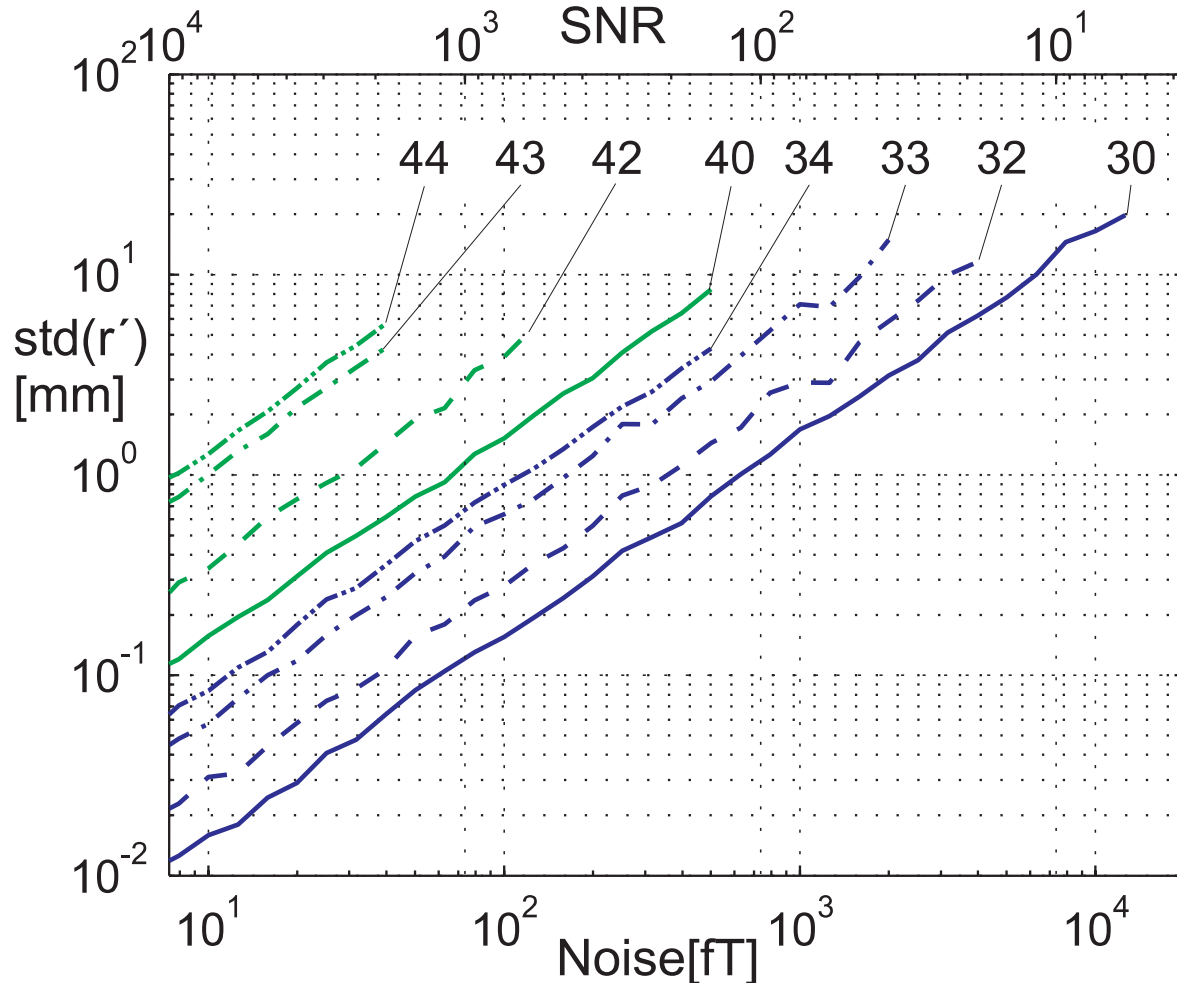
- Dipole with $20\mu\text{Am}^2$, 300mm below sensor level
- Gaussian noise
- Variation of multipole expansion order

Simulation setup



Simulations

Localization error as a function of noise



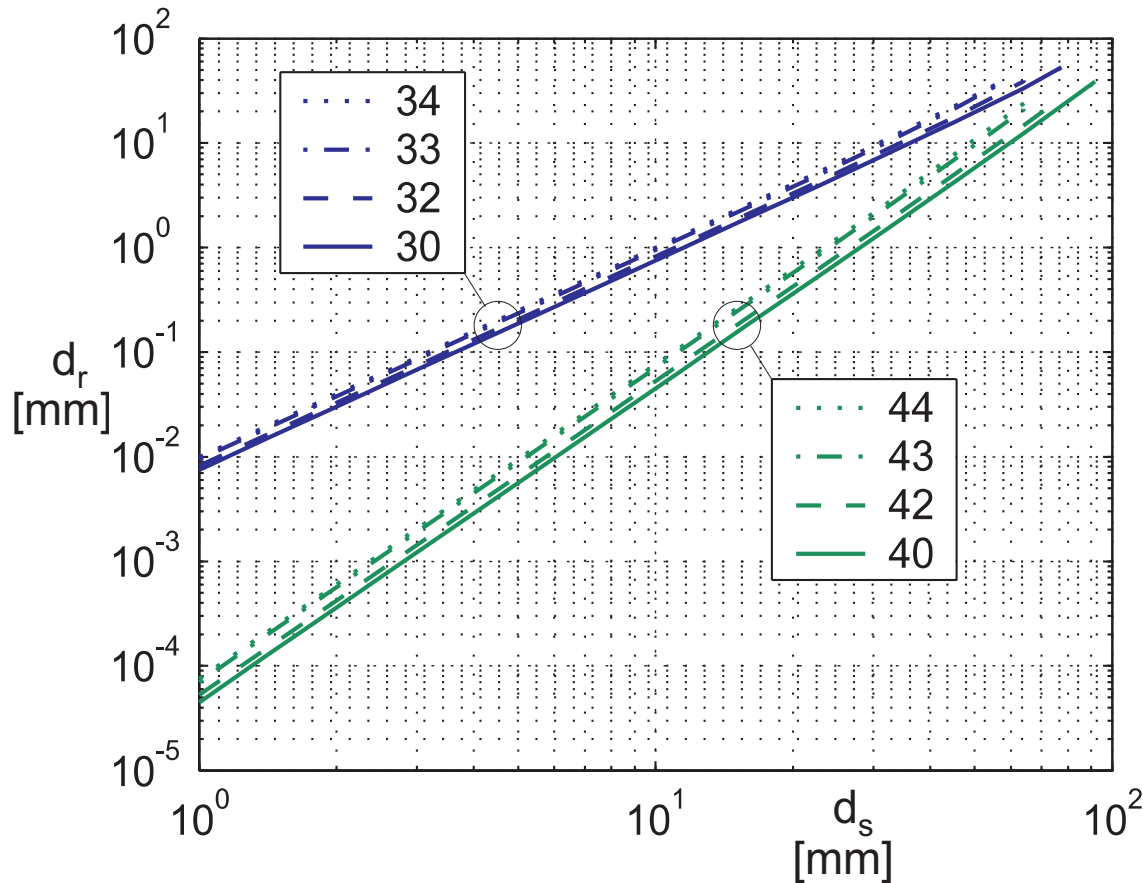
Marker strength $20\mu\text{Am}^2$
Marker pos $z = -300\text{mm}$

100 repeated runs per
data point

2 ... Dipole, 3 ... Dipole
and Quadrupole,
4 ... Dipole, Quadrupole
und Octupole
1st number: inner
2nd number: outer
multipole

Simulations

Localization error depending on the starting point distance d_s for one iteration



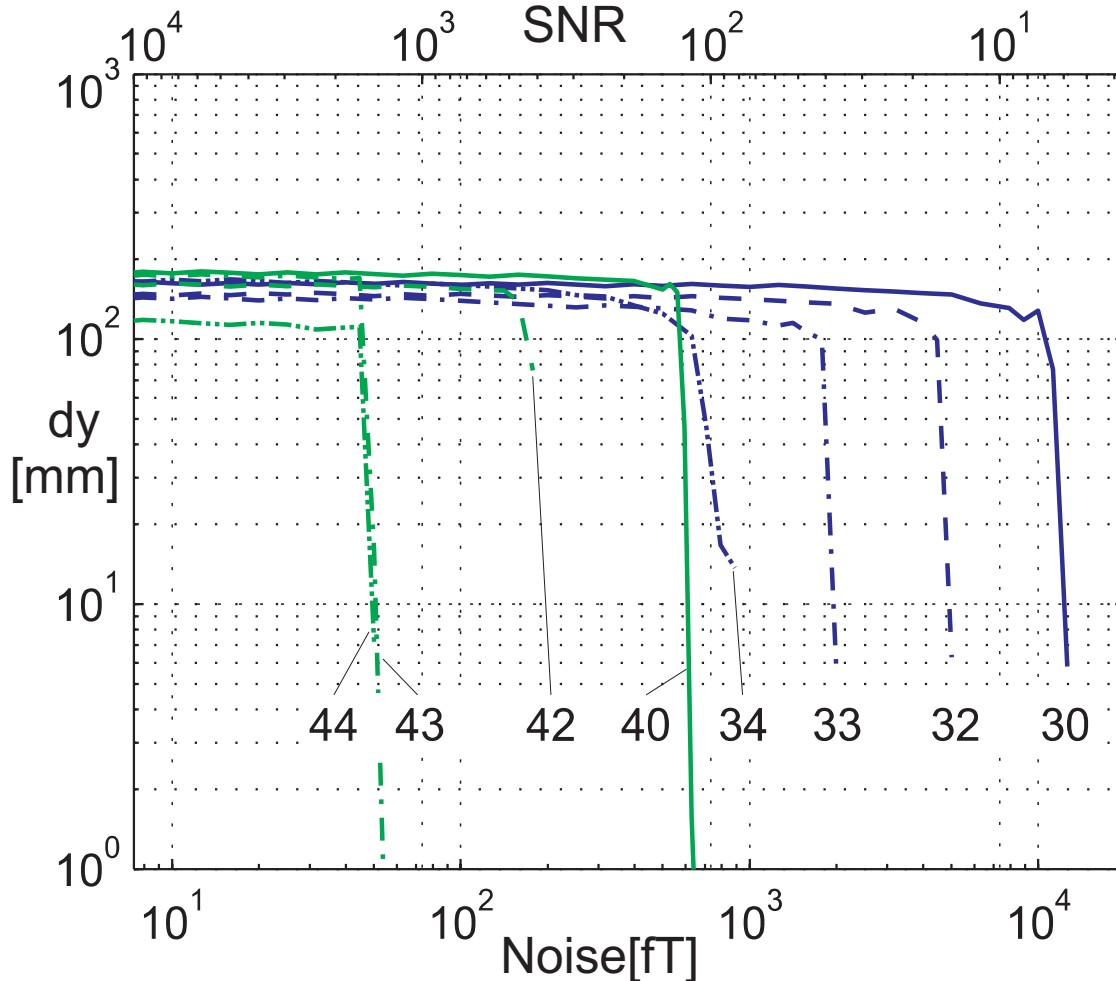
Marker strength $20\mu\text{Am}^2$
Marker pos $z = -300\text{mm}$

100 repeated runs per
data point

2 ... Dipole, 3 ... Dipole
and Quadrupole,
4 ... Dipole, Quadrupole
und Octupole
1st number: inner
2nd number: outer
multipole

Simulations

Convergence distance depending on noise level



Marker strength $20\mu\text{Am}^2$
Marker pos $z = -300\text{mm}$

100 repeated runs per
data point

2 ... Dipole, 3 ... Dipole
and Quadrupole,
4 ... Dipole, Quadrupole
und Octupole
1st number: inner
2nd number: outer
multipole

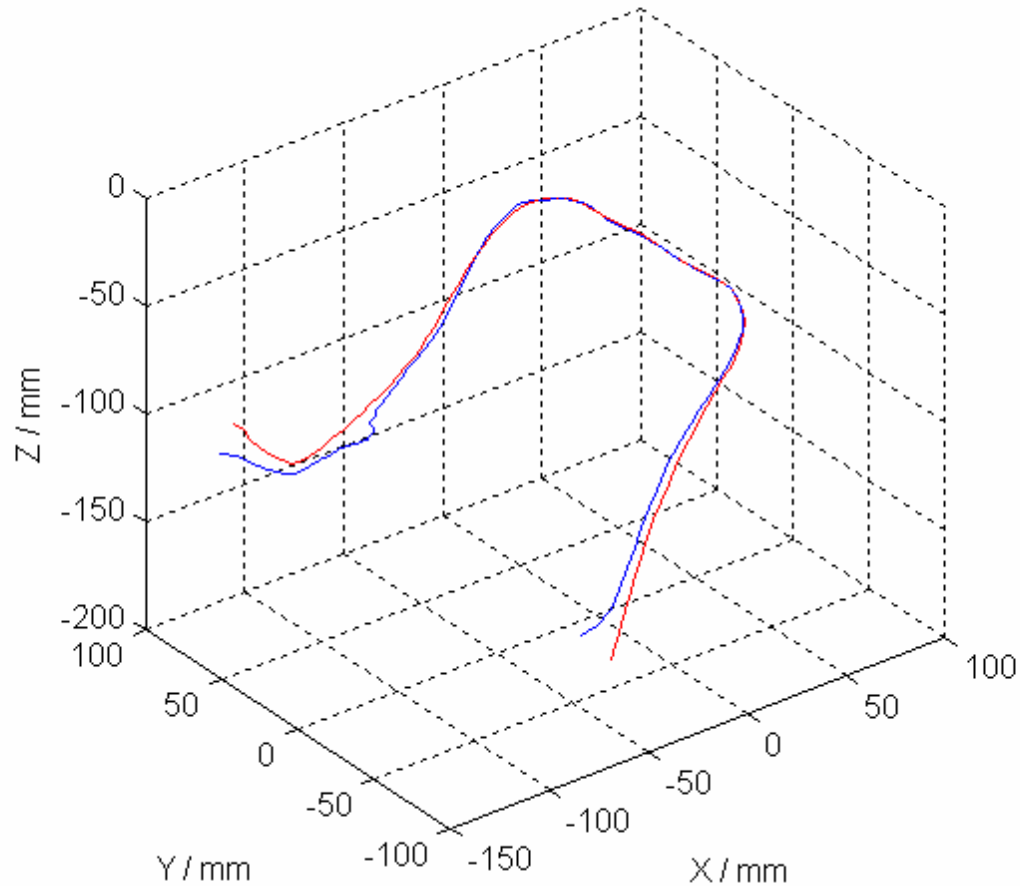
Measurement with glass phantom

Marker in fluid (sucrose)
under measurement system



Marker

Measurement with glass phantom



Clinical study with magnetically marked tablets

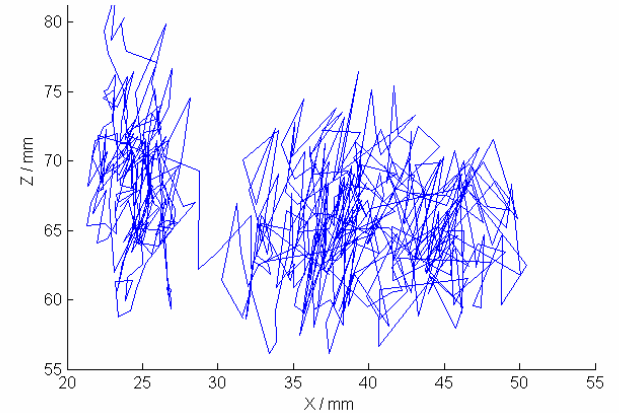
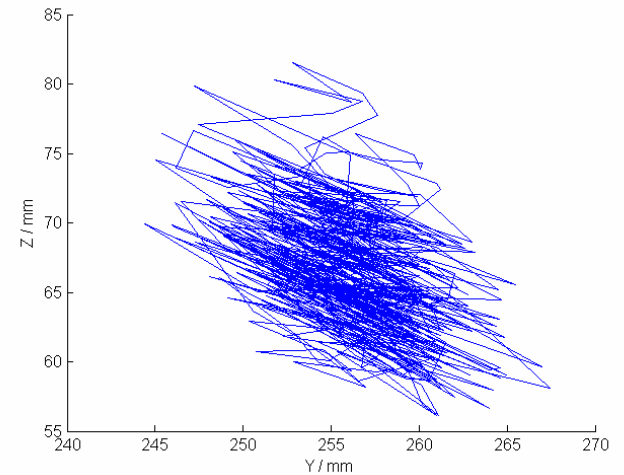
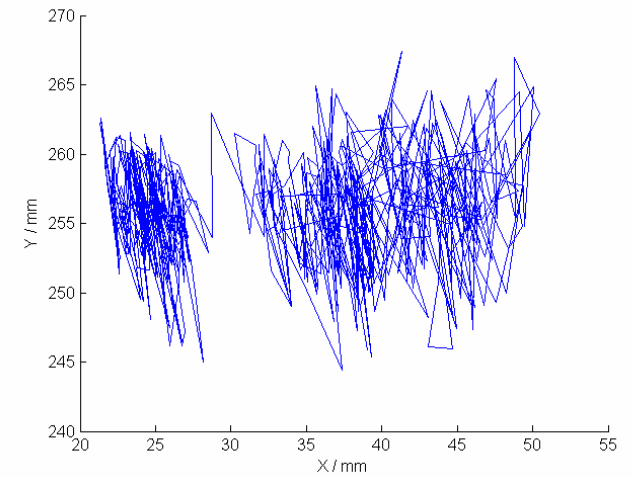
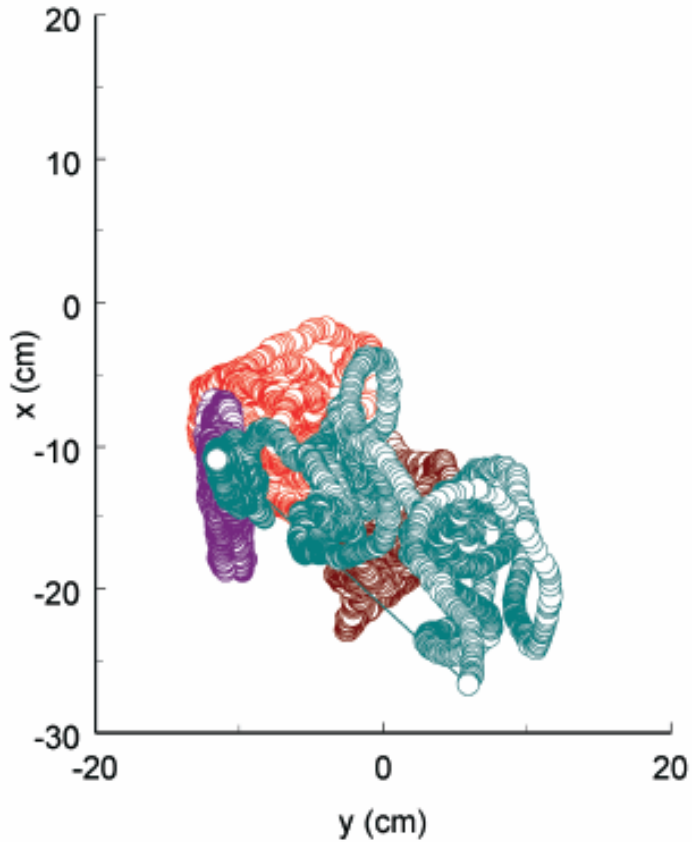


Clinical study with magnetically marked tablets

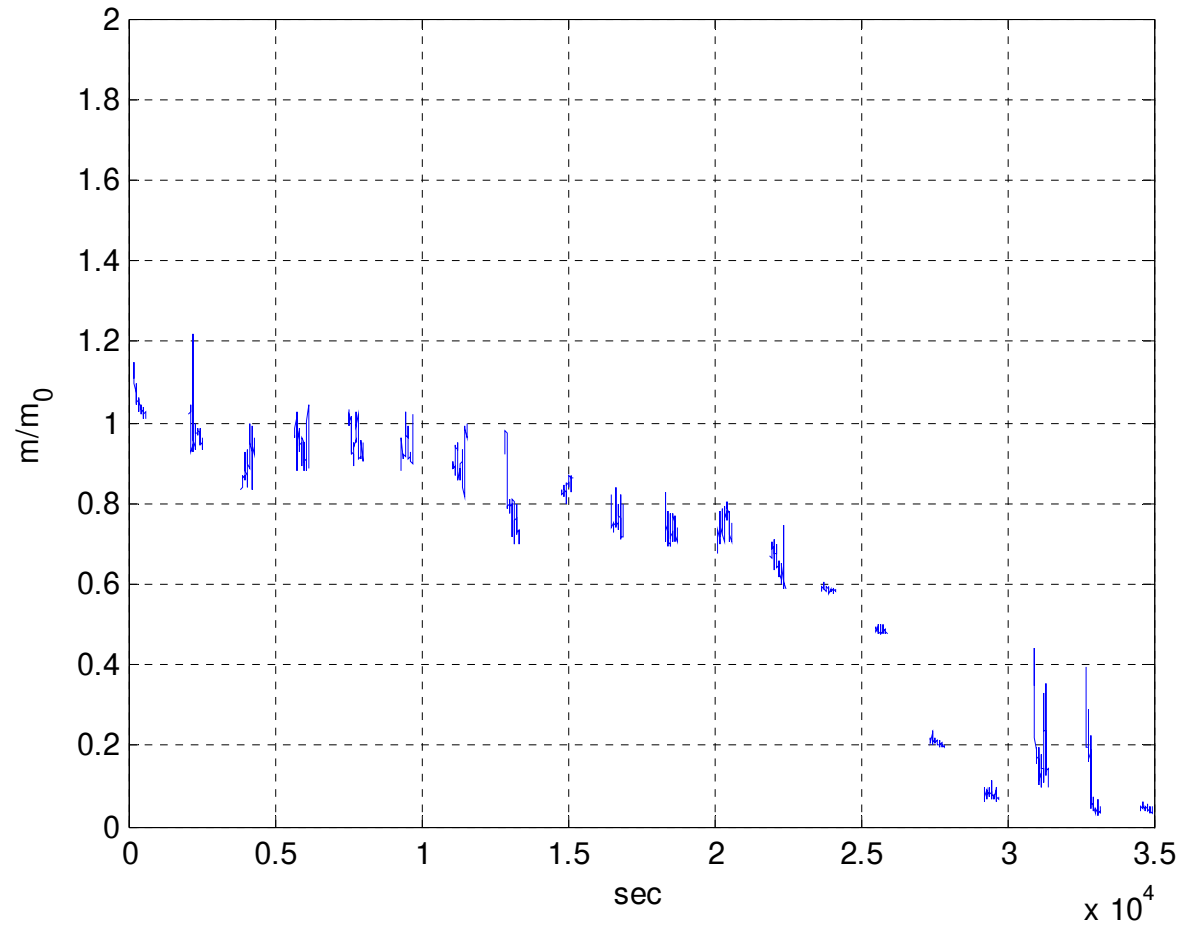
- Determination of drug disposal in the intestine
- Test- and reference tablets
- Two sets of measurement on 12 probands
- 10-min for single measurement, 30 min inter-measurement time, total time about 12 hours
- 2 probands per day, blood control every 30 min

Localization results

- one measurement, 1S/s
- Respiratory movements
- larger movement in the colon



Marker moment for one series



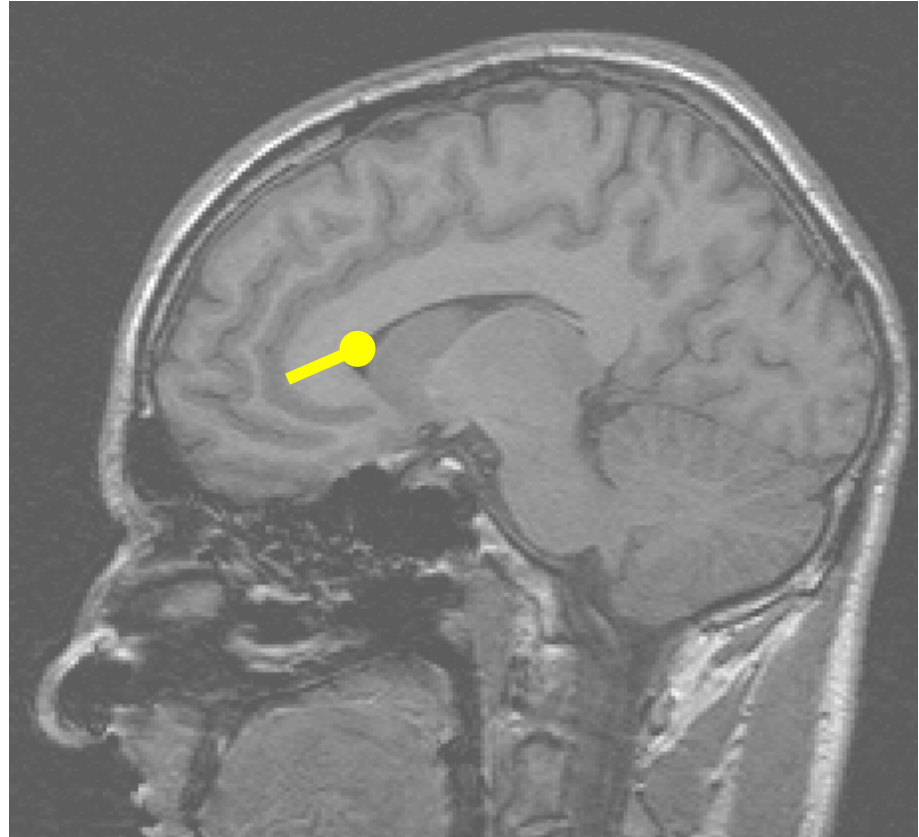
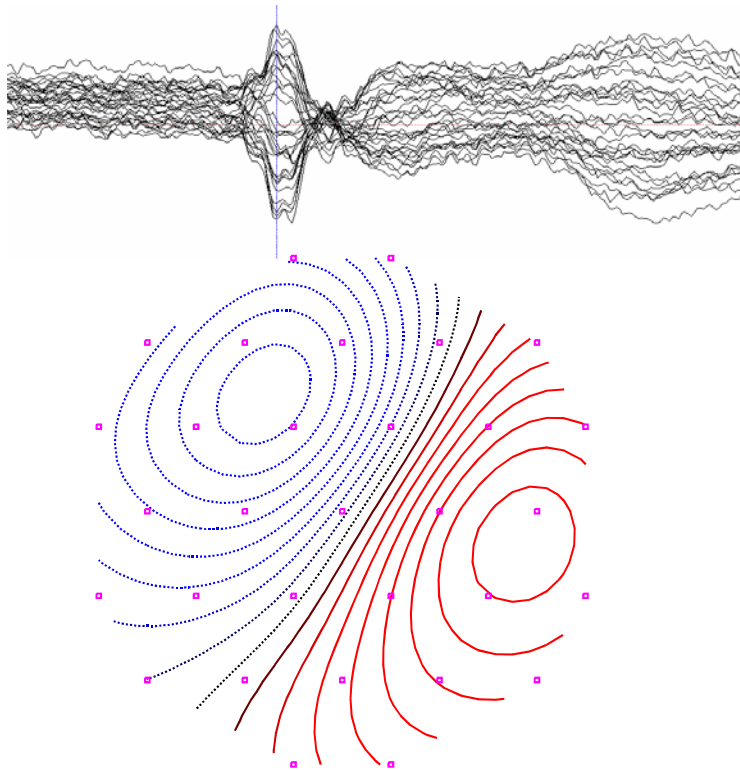
Summary

- Fast online method: max. 3 iterations for each localization
- SNR better 100 is recommended
- Inner oktupole not used because of high sensitivity to noise
- Starting point within about 10 cm of true location

Overview

1. Introduction
2. Localization of magnetic markers in the alimentary tract
3. **The influence of forward model conductivities on EEG/MEG source reconstruction**
 1. Finite Element Modeling
 2. Animal sensitivity analysis
 3. Human sensitivity analysis
4. Optimization of magnetic sensor arrays for magnetocardiography
5. Validation of source reconstruction procedures

Introduction



- How does volume conduction influence source estimation?
- How does anisotropy influence source estimation?

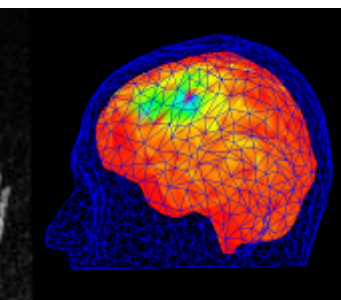
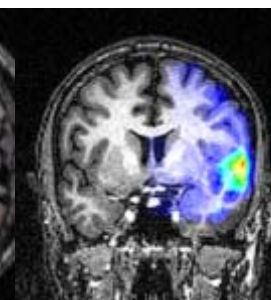
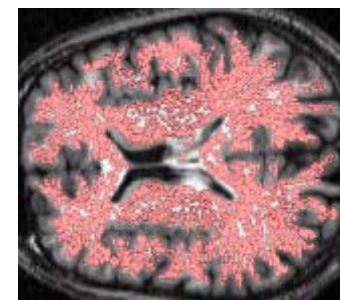
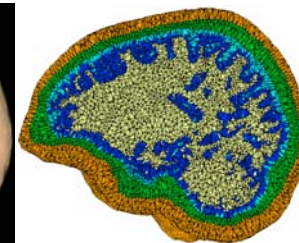
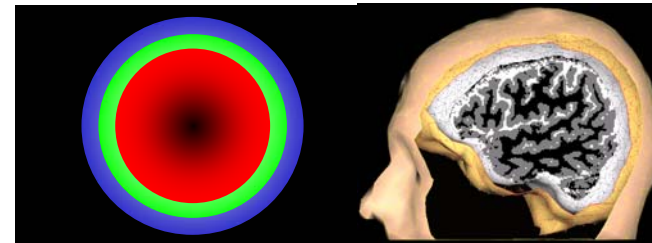
Image Registration (T1, T2, PD)

Segmentation

Mesh Generation BEM/FEM

Forward toolbox
Inverse toolbox

Visualisation



Galerwin



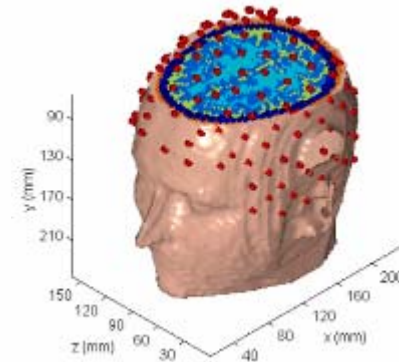
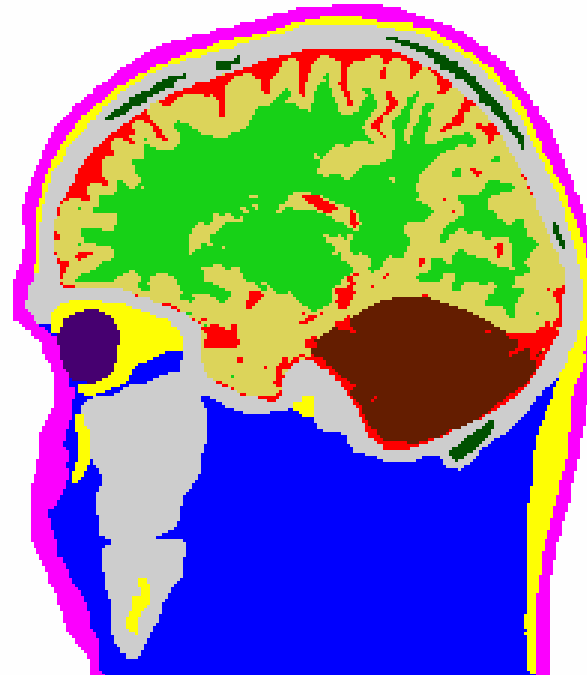
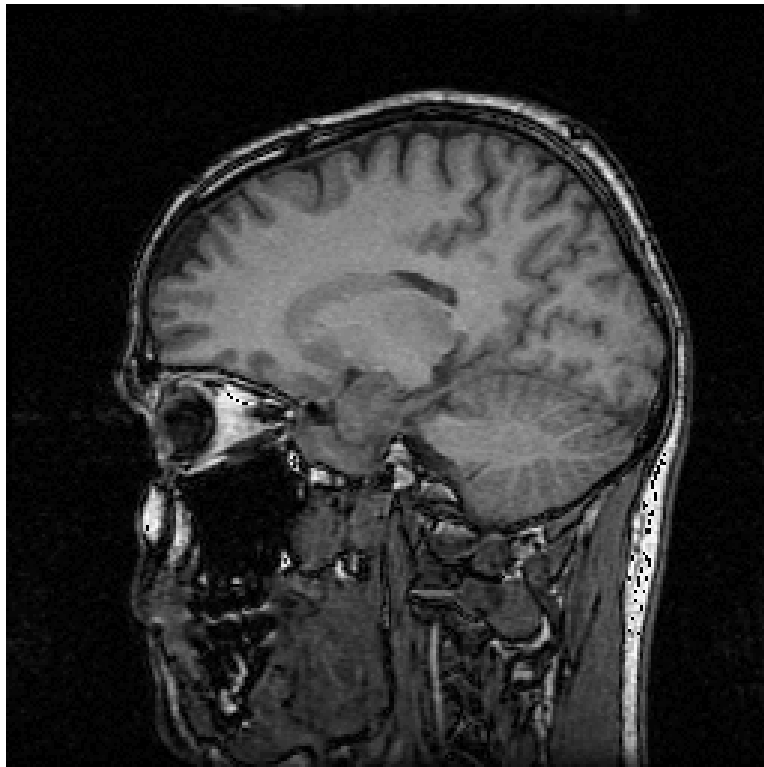
Institut für Biomedizinische
Technik und Informatik

T1 weighted MR data:

- 1.6 mm slice thickness,
- 102 slices,
- 1 mm x 1 mm pixel size

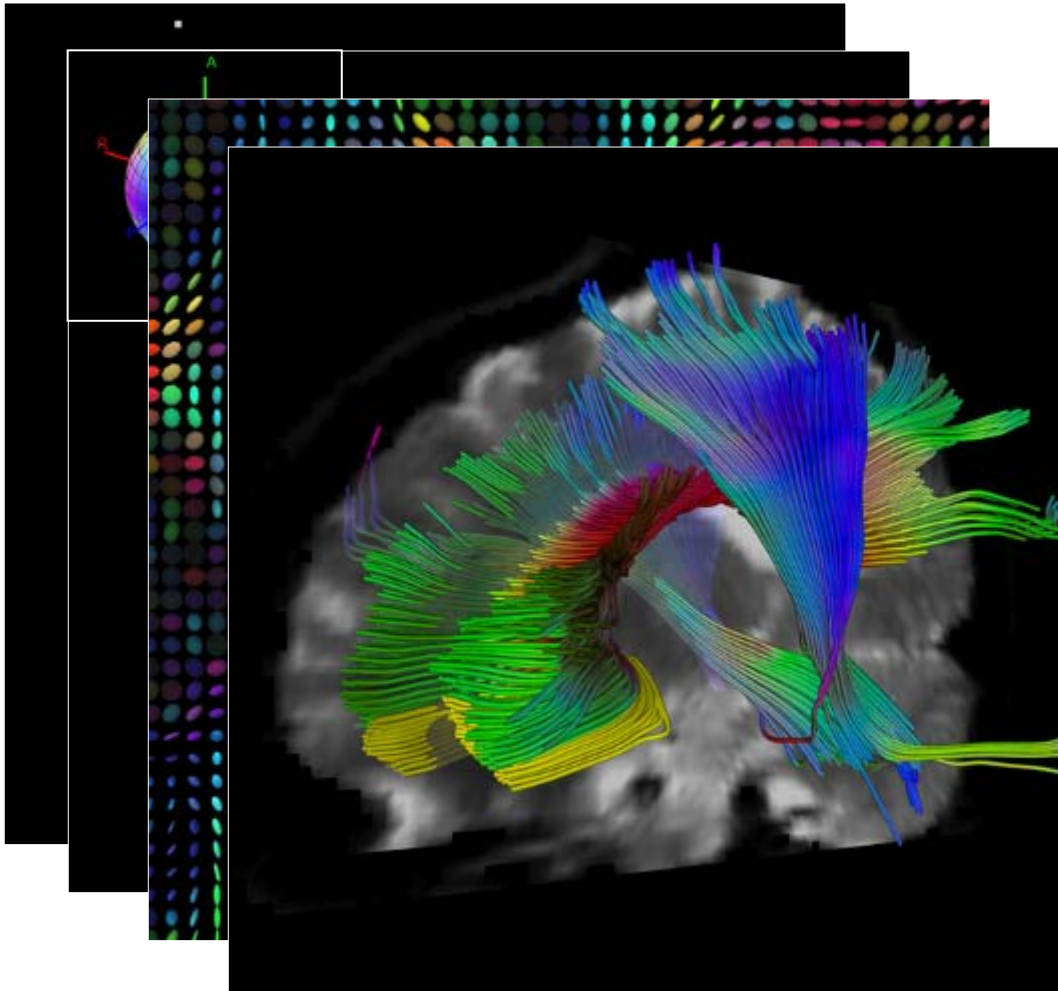
FEM model cross section:

- resolution of 1 mm x 1 mm x 3.2 mm,
- 1,456,069 hexahedral elements (voxels)
- adaptive JCG solver



Conductivity and anisotropy data

Human Diffusion Tensor Imaging



Anisotropy map (FA)

Anisotropy map color coded

Diffusion tensor as ellipsoid

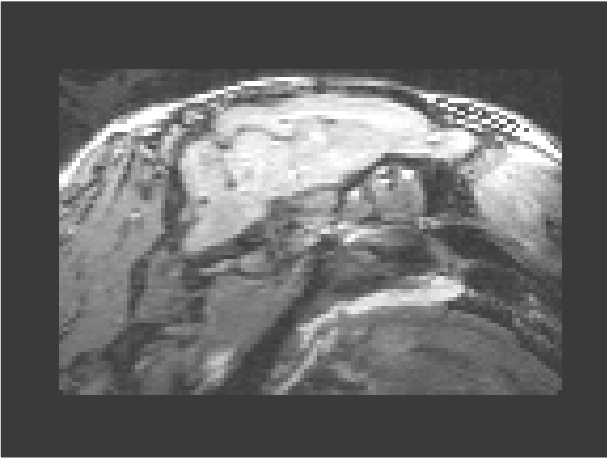
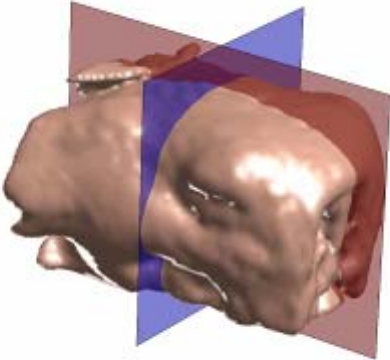
Fiber tracking (main direction of strong anisotropic tensors)

Conductivity and anisotropy data

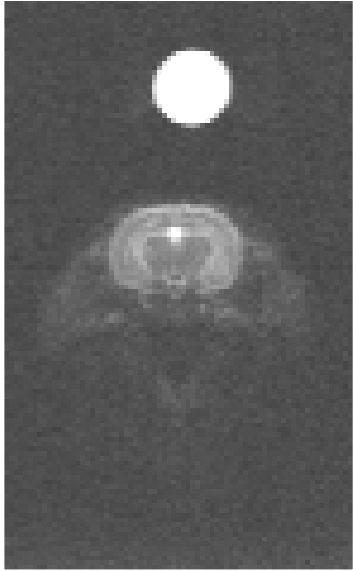


Institut für Biomedizinische
Technik und Informatik

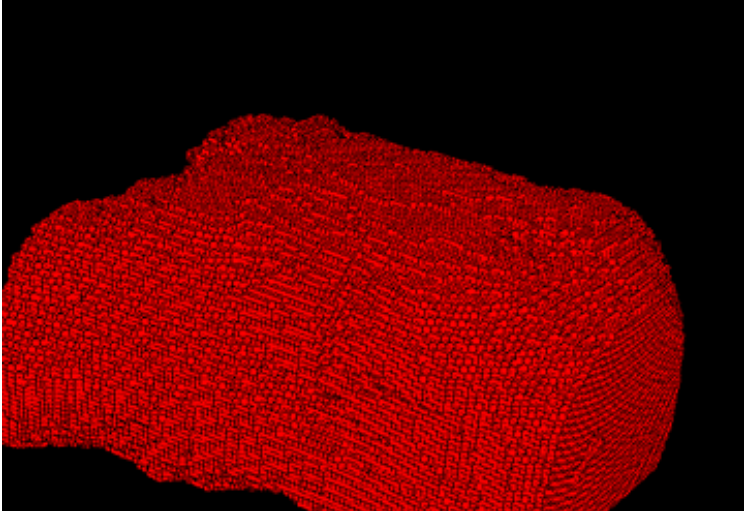
Rabbit imaging



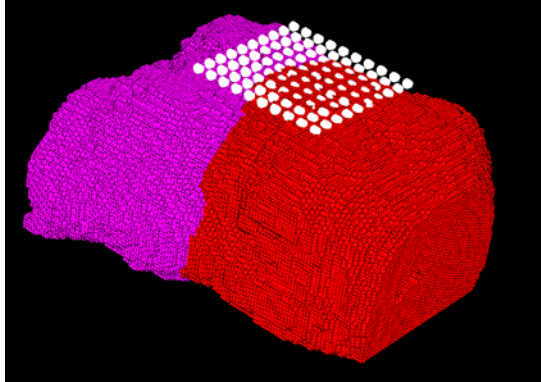
Flash3D T1
(isotropic resolution 0.625 mm)



TSteam - DTI



633172 cubic
elements (0.6mm)

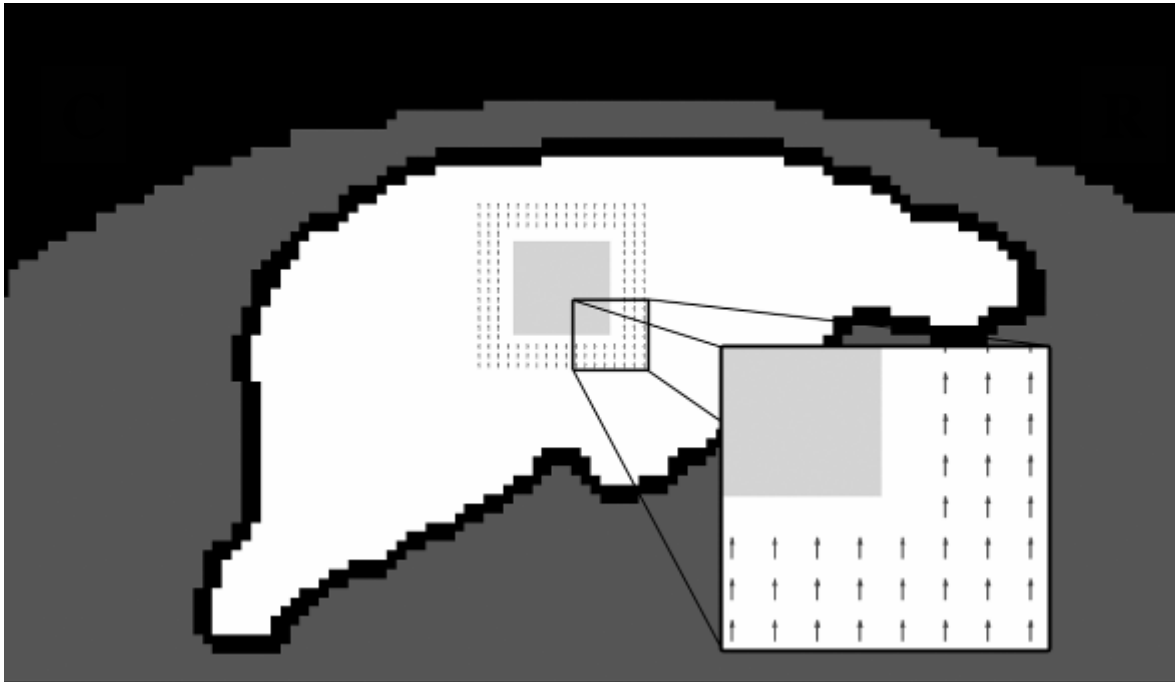


Animal sensitivity analysis

Simulations with a block of white matter



Institut für Biomedizinische
Technik und Informatik



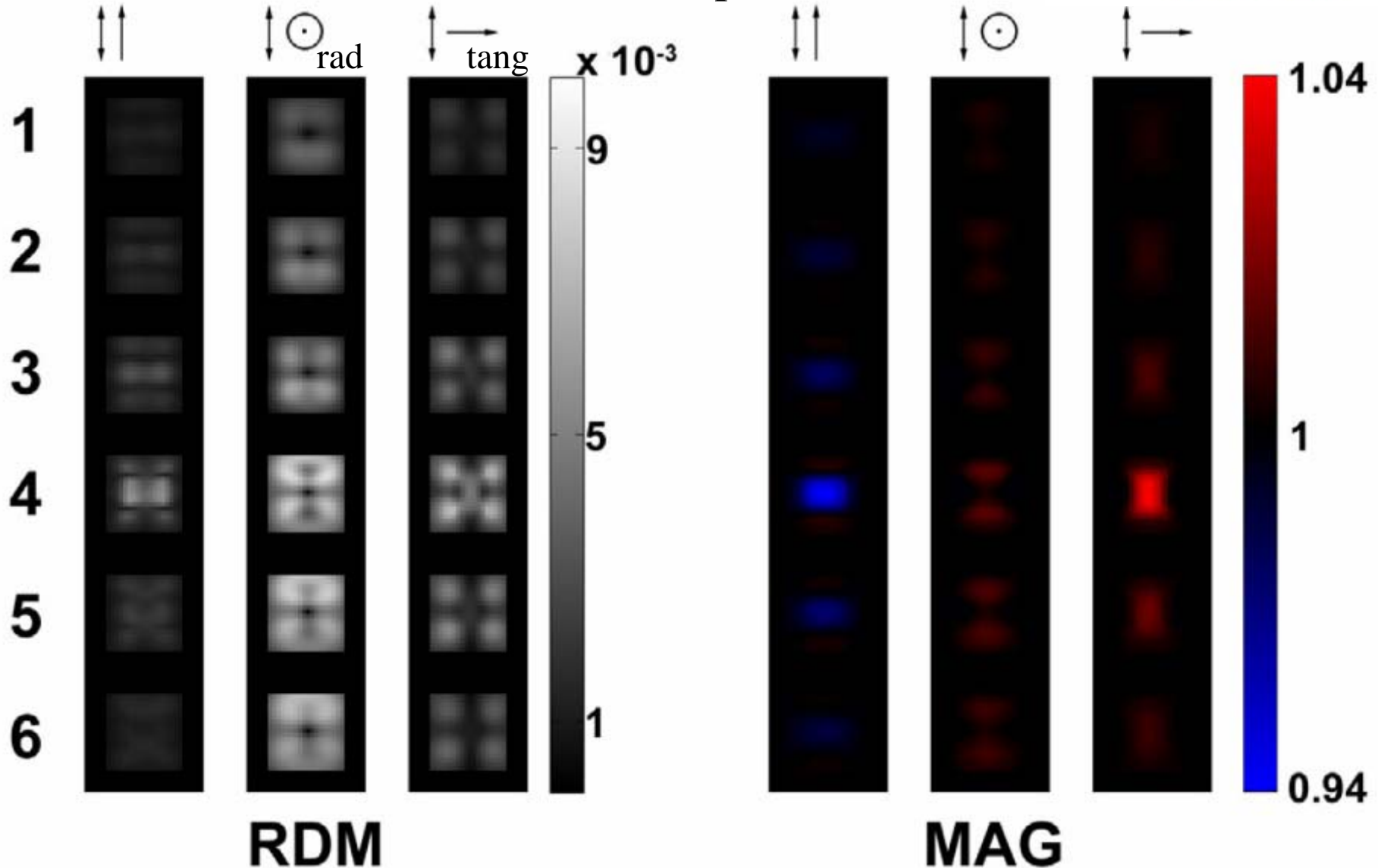
Sagittal slice with
4 tissue types:

- skin
- skull
- gray matter
- artificial white matter block

- source space with 3 layers of dipoles around the anisotropic block
- dipole orientation left/right, rostral/caudal, and inferior/superior
- anisotropic conductivity of 1:10 in caudal-rostral orientation

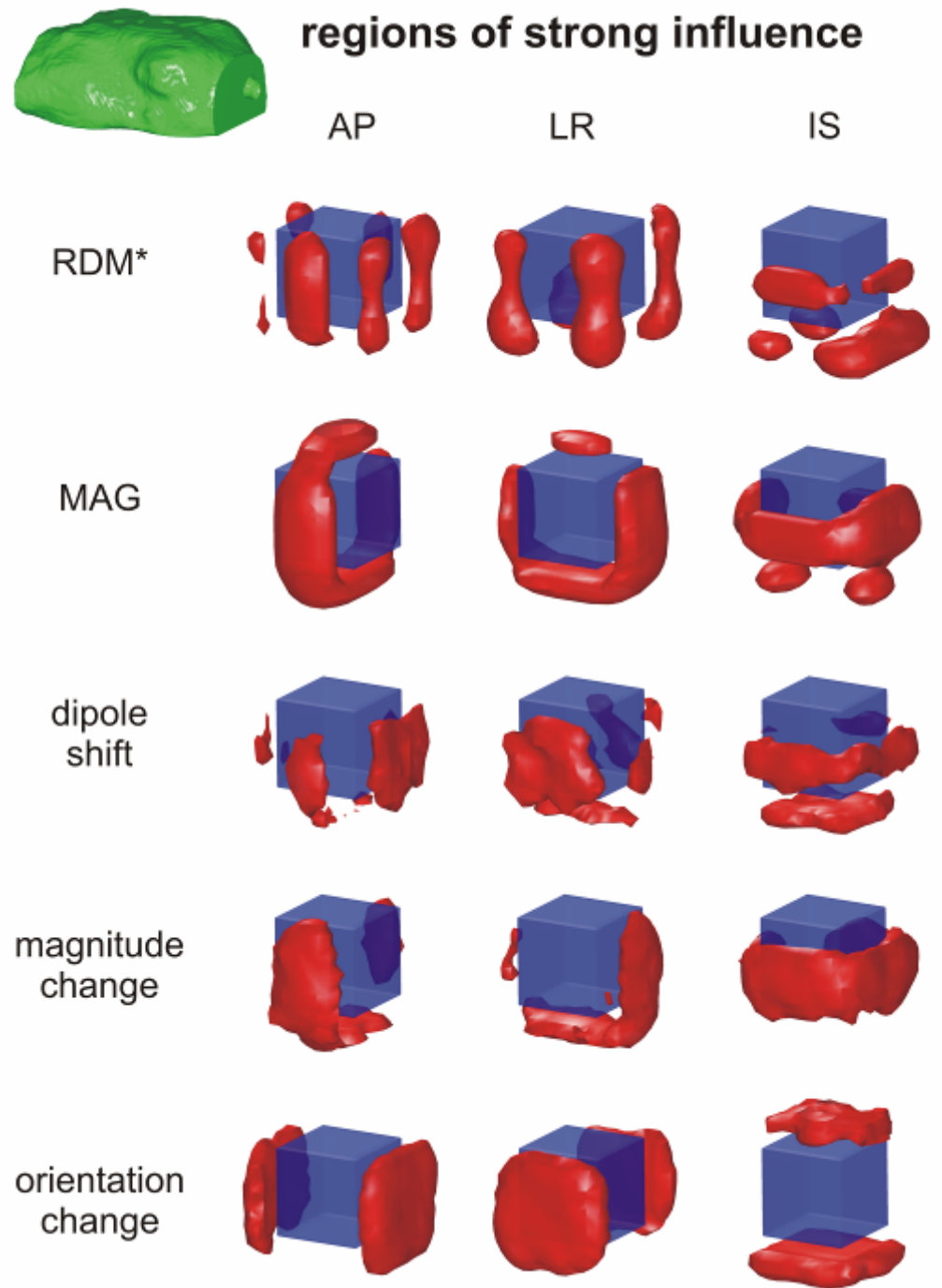
Animal sensitivity analysis

Differences in the forward computations

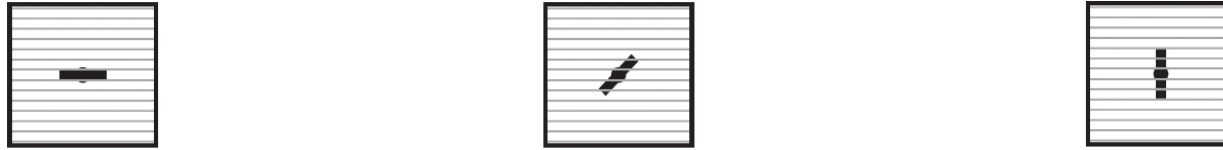


Simulations with a block of white matter

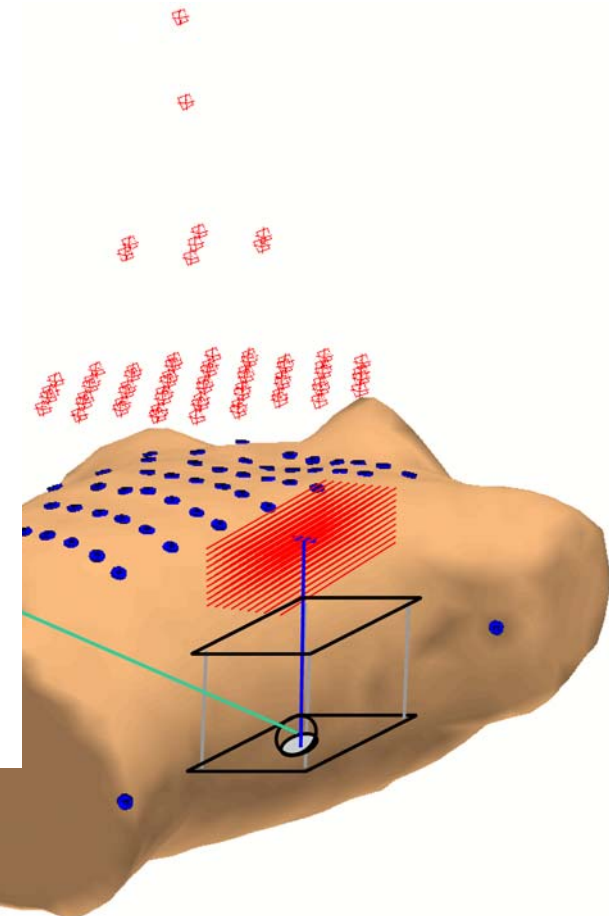
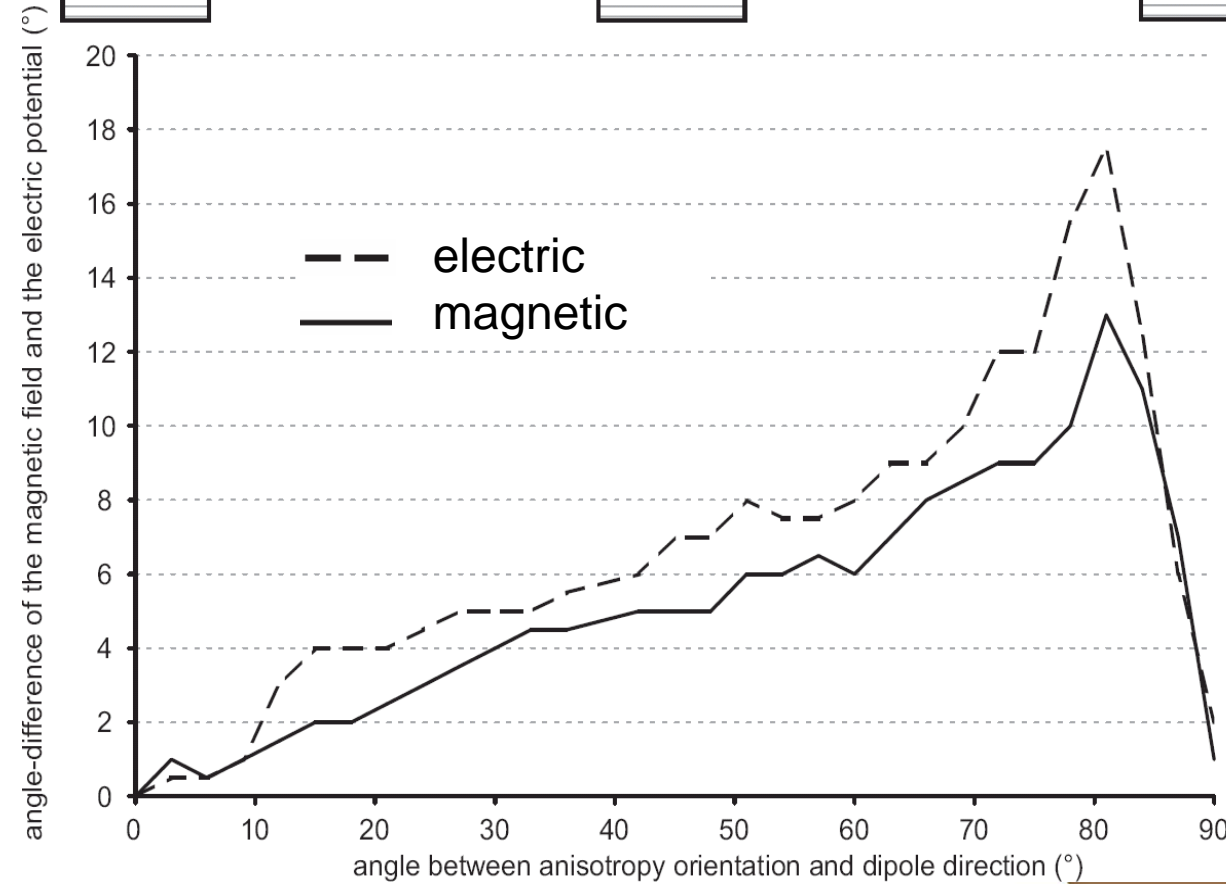
Values above the 0.8 percentile for RDM*, MAG, dipole shift, magnitude change and orientation change are visualized by red surfaces.



Experimental validation

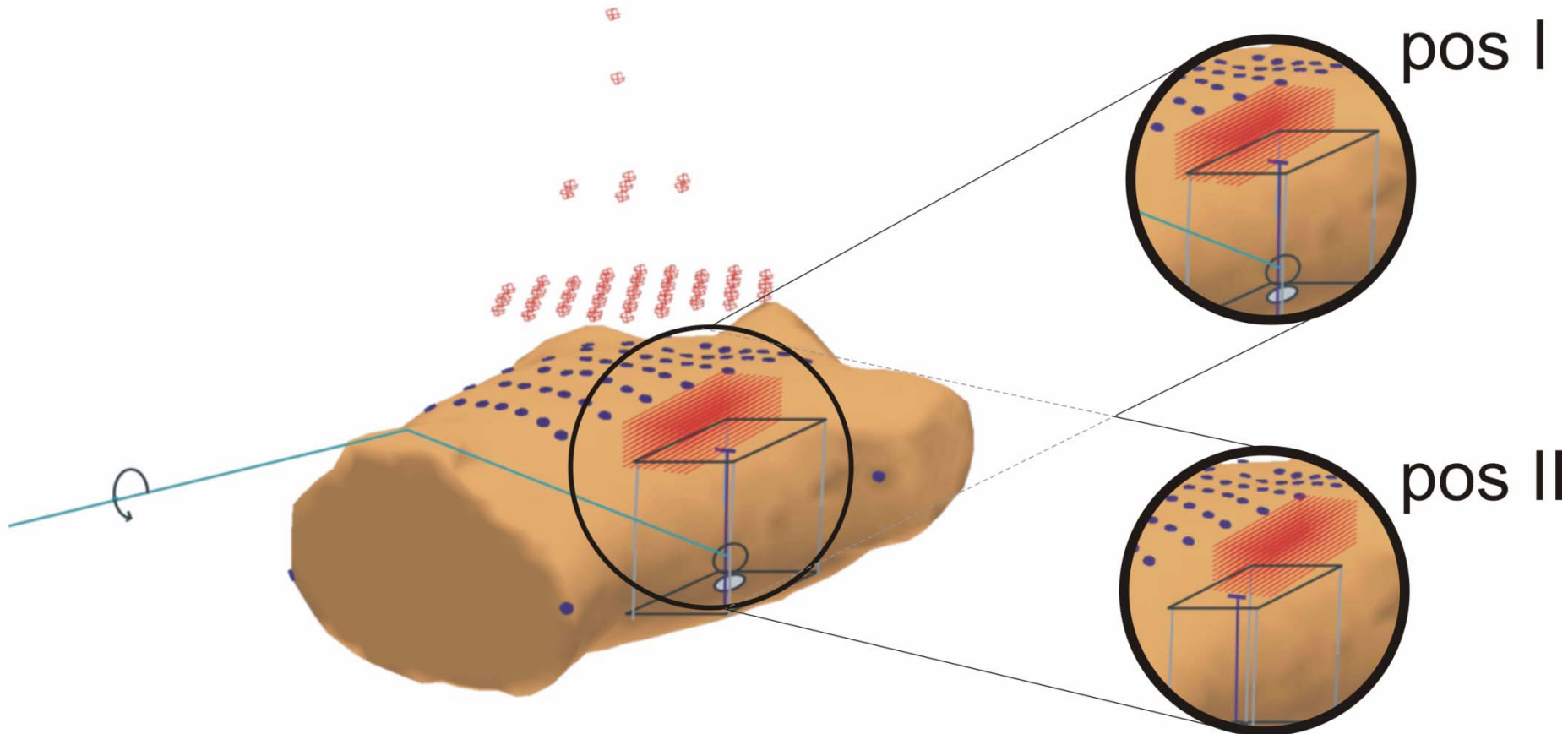


Anisotropic block
in a torso phantom

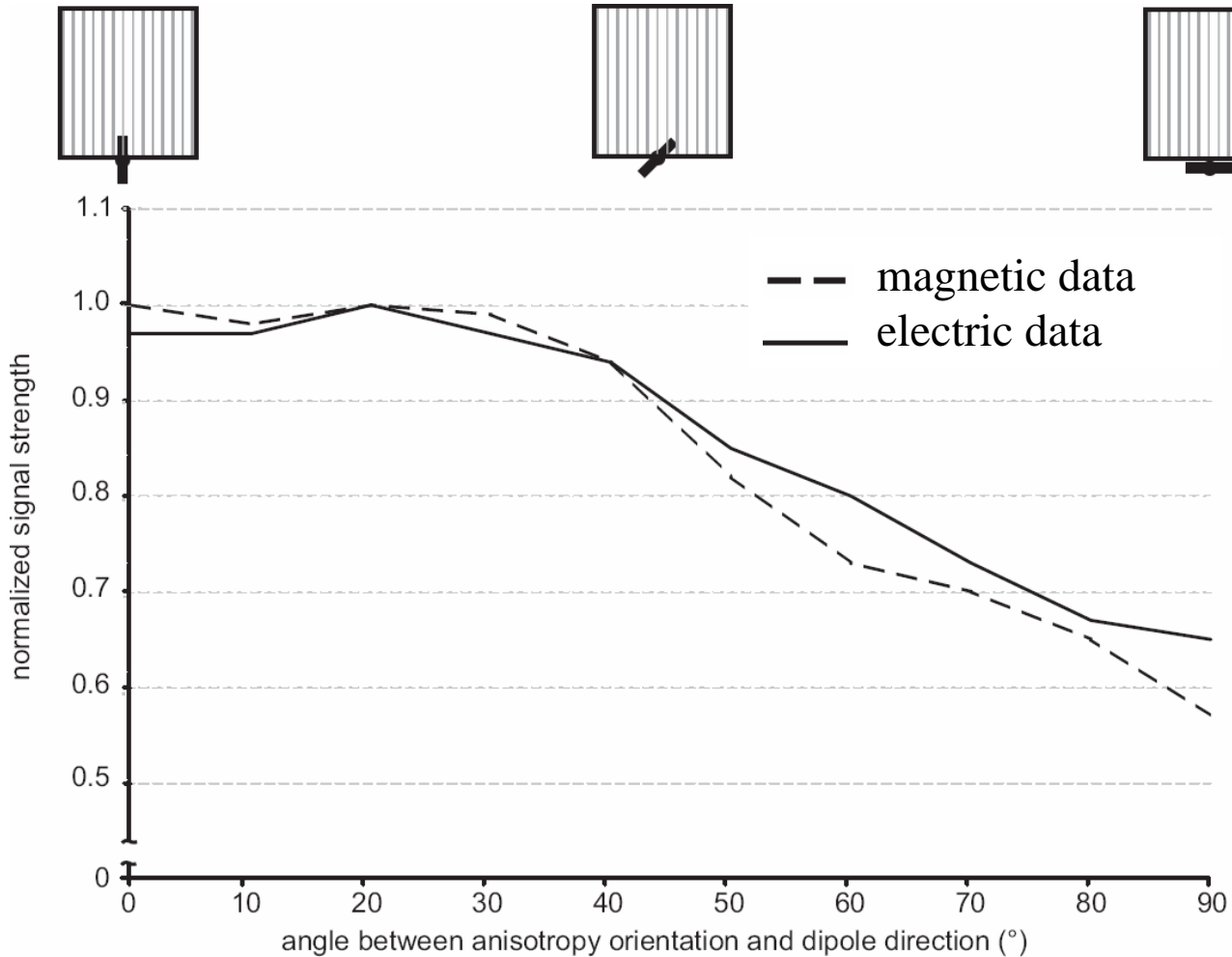


Experimental validation

Anisotropic block in a torso phantom



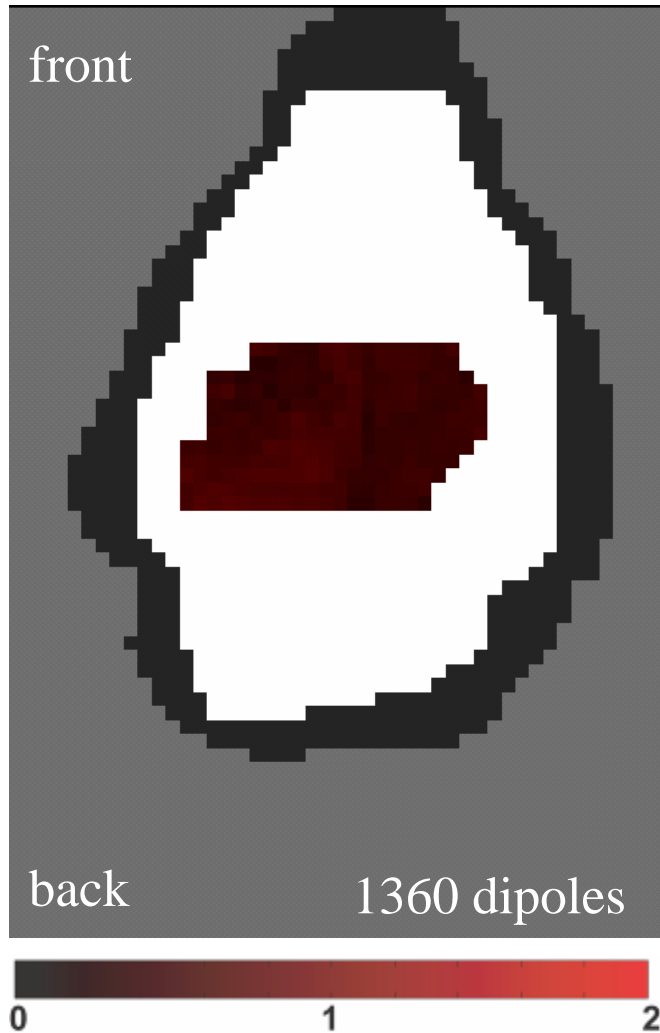
Experimental validation



Anisotropic block
in a torso phantom

Animal sensitivity analysis

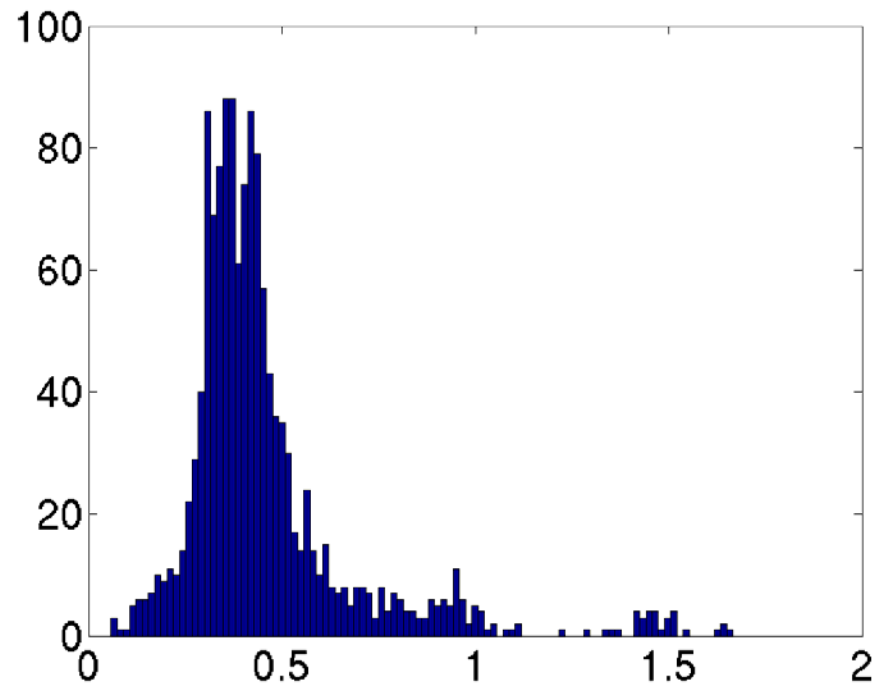
Simulations with measured conductivity tensors



Source localization error

Forward computation:
anisotropic model

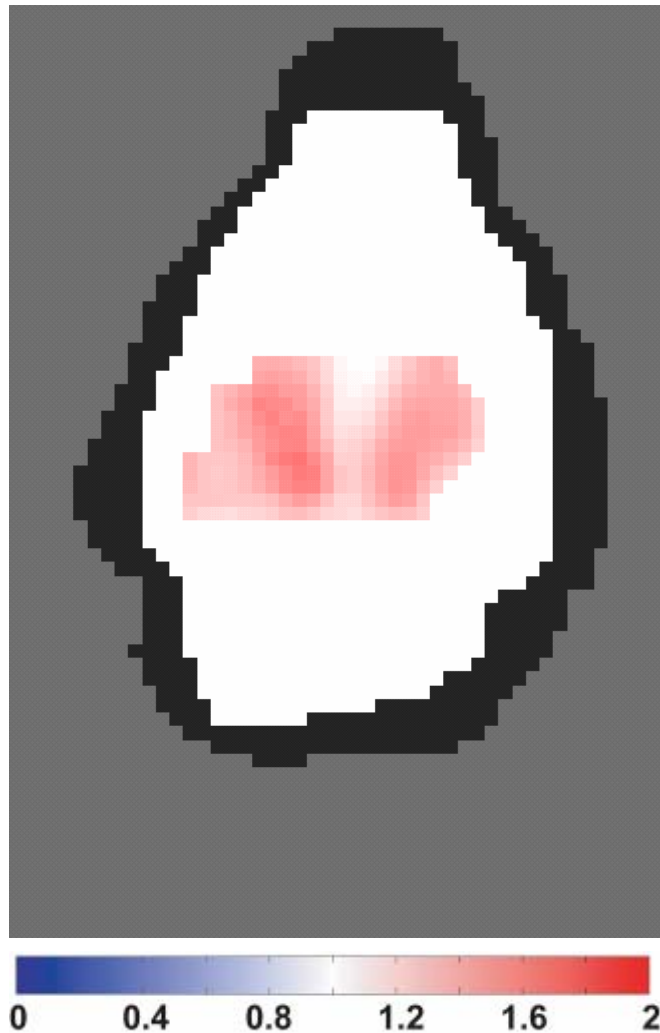
Inverse: isotropic model



Histogram of the dipole shift

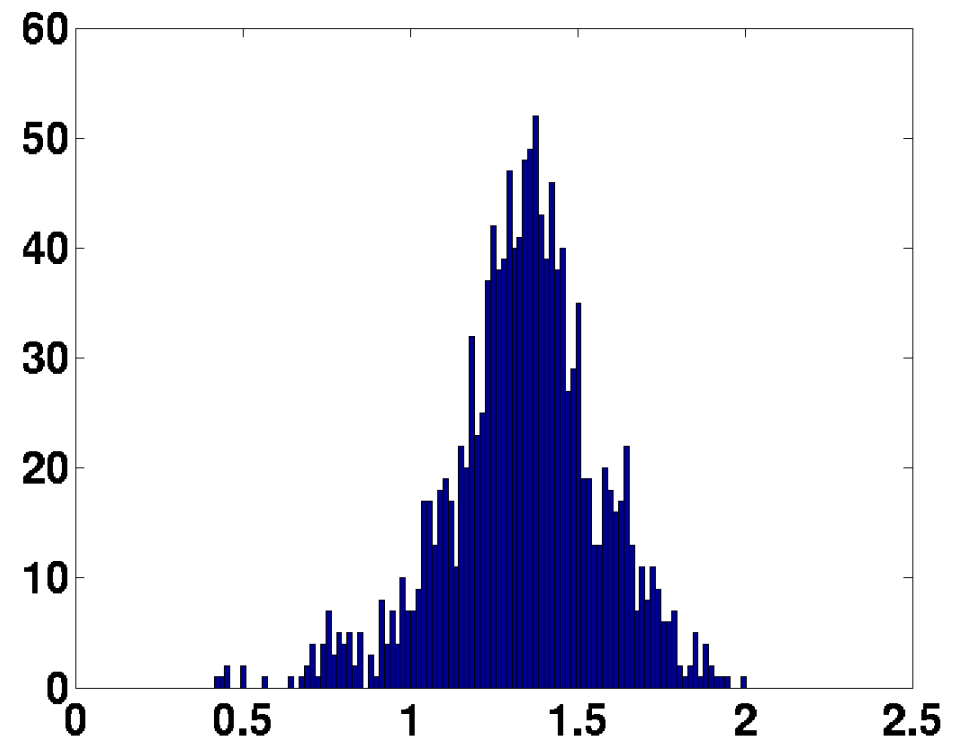
Animal sensitivity analysis

Simulations with measured conductivity tensors



Magnitude change (relative to 1)

Dipole magnitude estimation error

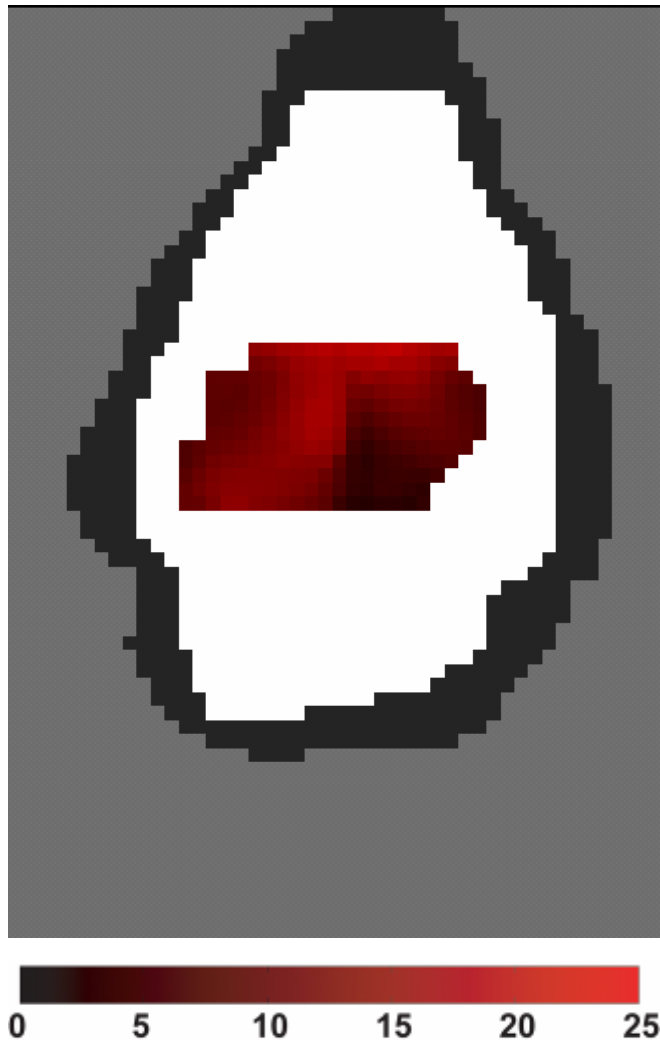


Histogram of the dipole magnitude errors

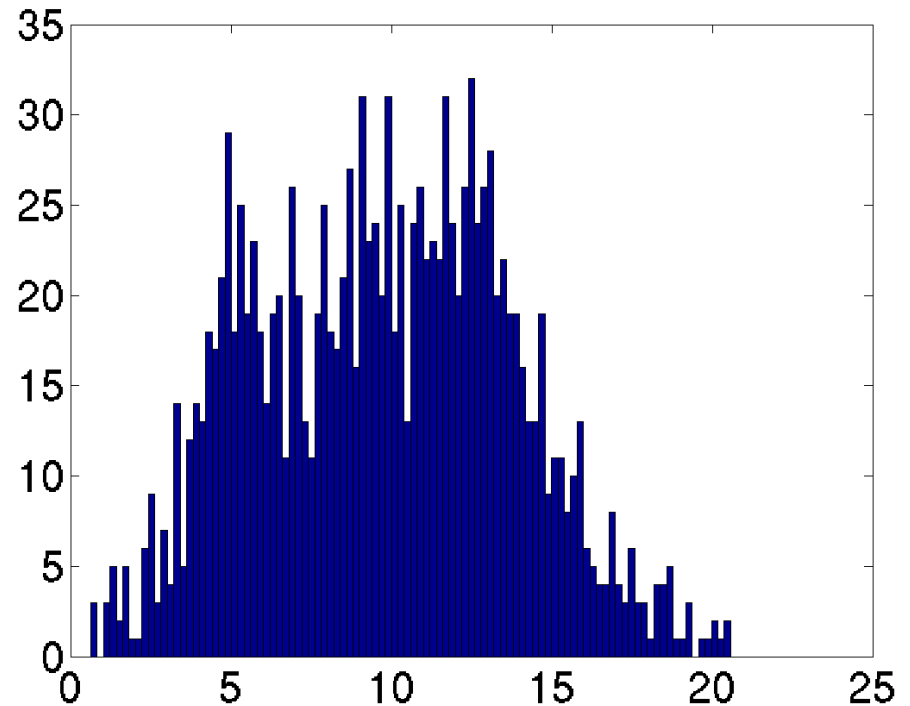
Animal sensitivity analysis

Simulations with measured conductivity tensors

Dipole orientation estimation error



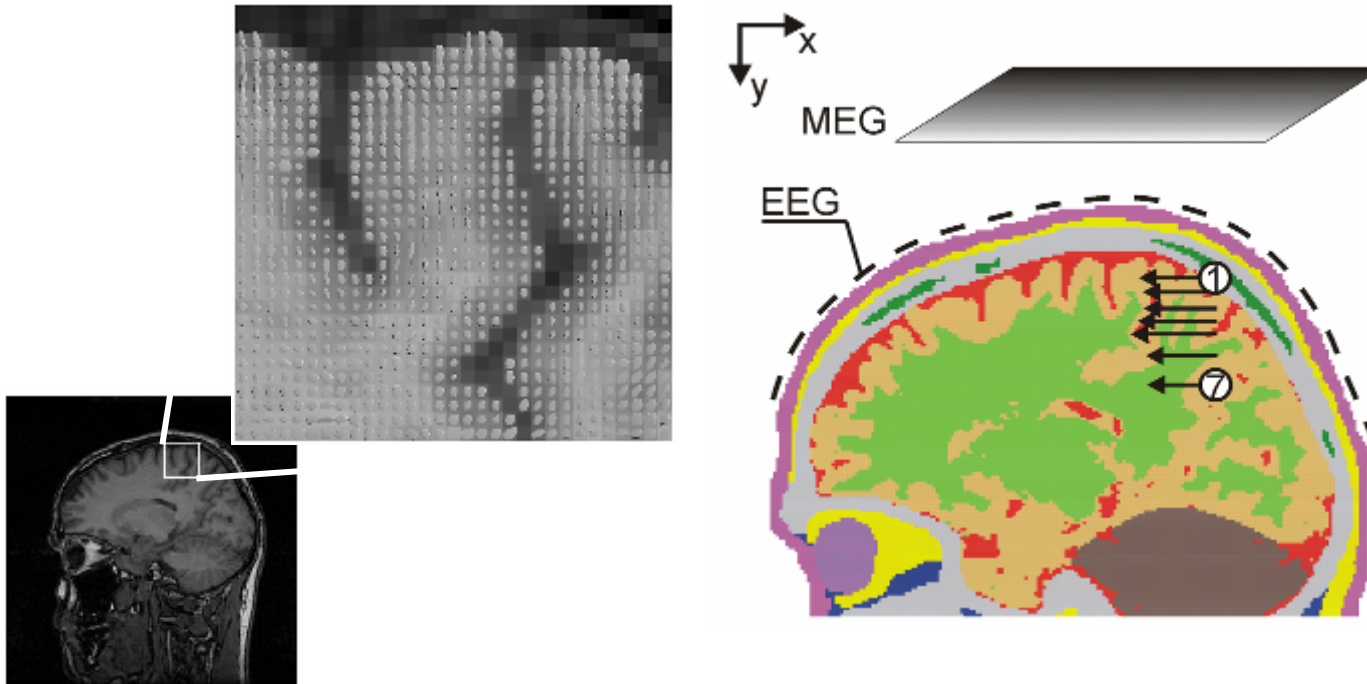
Orientation change in deg



Histogram of the dipole orientation errors

Sensitivity analysis

Forward simulations with isotropic and anisotropic human head models

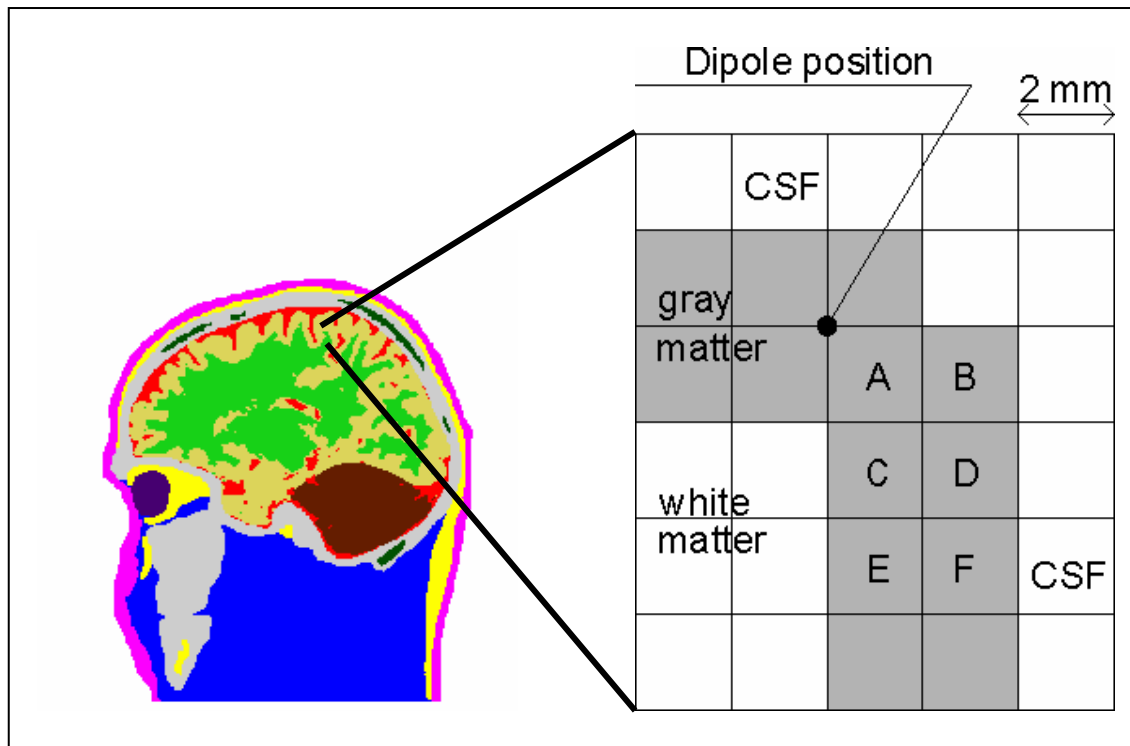


Results:
Correlation:
above 0.98
Magnitude:
more than 50%
change

Tissue anisotropy seems to have a minor influence on source localization but a major influence on dipole strength estimation.

Sensitivity analysis

Simulations with conductivity changes of single voxels



Results:

Correlation:

Change in A: 0.98

Change B-F: >0.999

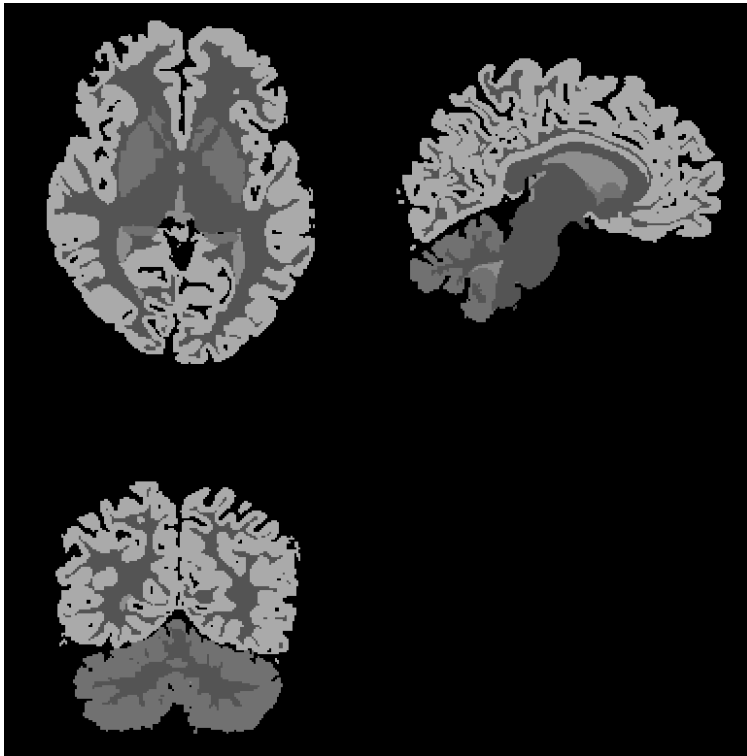
Magnitude:

Change in A: 2 - 60%

Change B-F: $< 1\%$

Conductivity changes in the vicinity of the dipole influence source estimation.

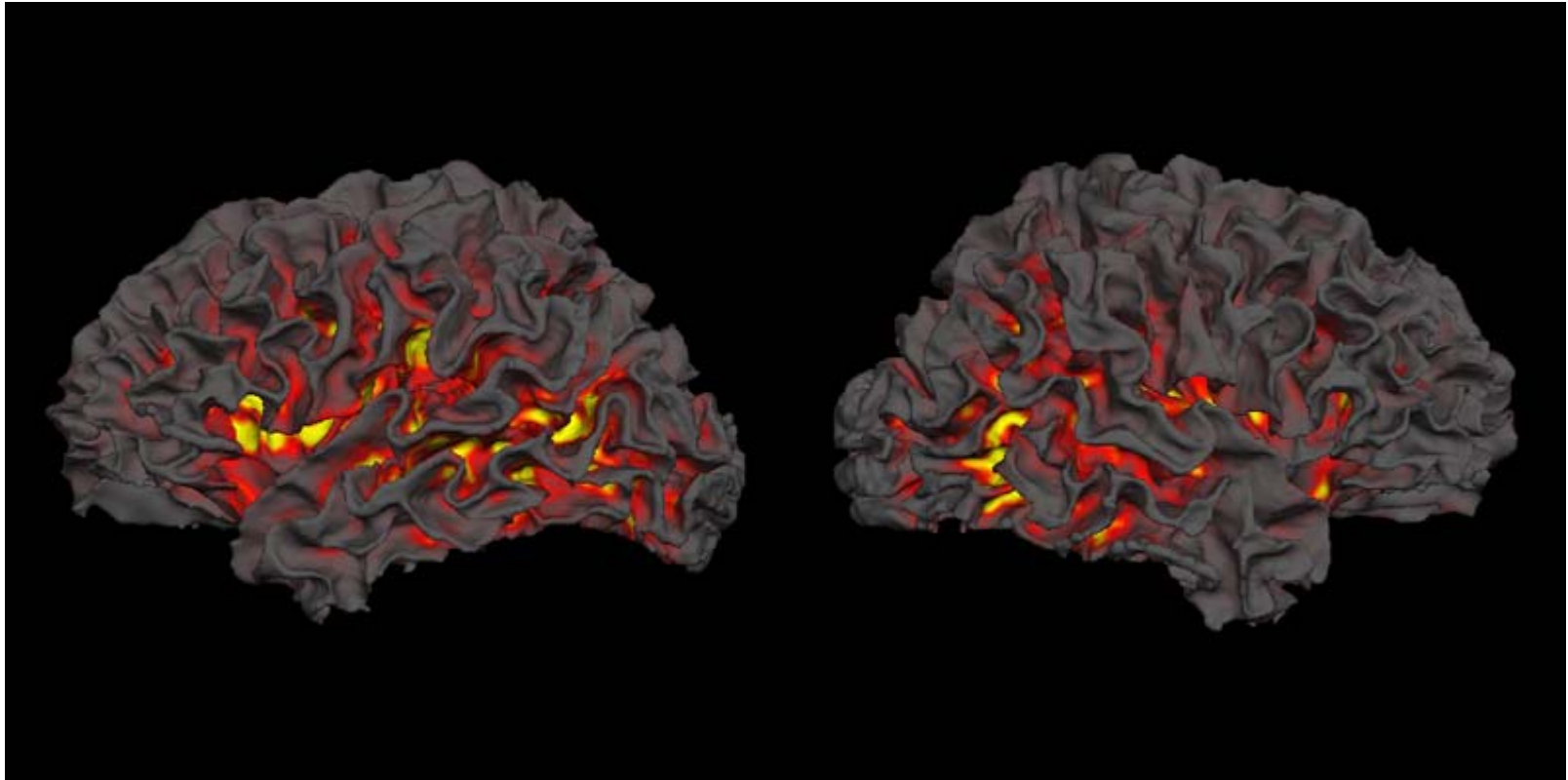
Human sensitivity analysis



- 5 tissue types
- 3.2 million cubic elements (1mm)
- 130 electrodes
- 25,000 dipoles perpendicular to cortical surface
- anisotropies of 1:2, 1:5, 1:10 and 1:100

Comparison of isotropic and anisotropic model output by RDM and MAG mapped to each dipole position

Human sensitivity analysis

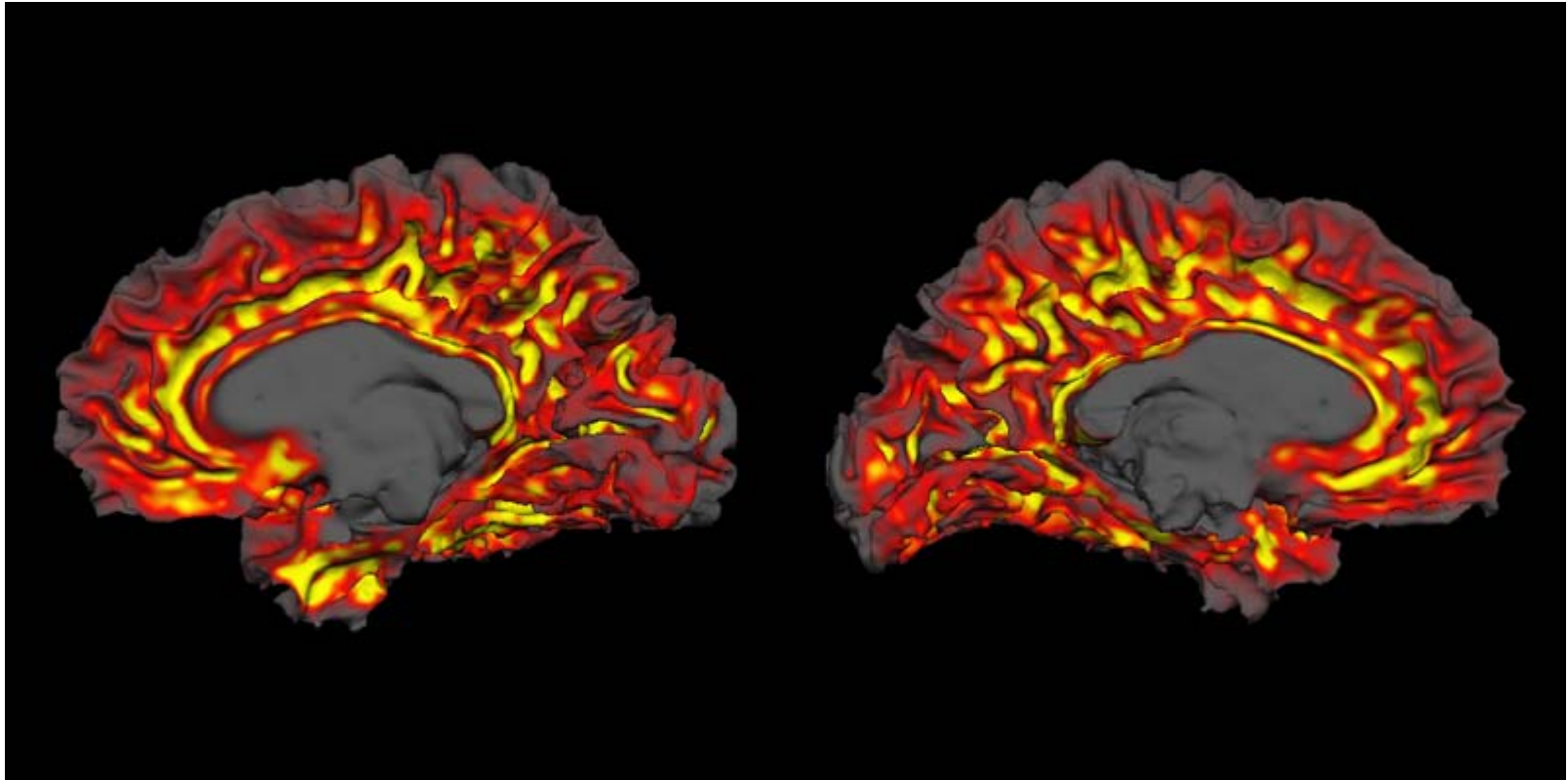


right hemisphere

left hemisphere

Relative Difference Measure – outside view

Human sensitivity analysis



right hemisphere

left hemisphere

Relative Difference Measure – inside view

Conclusions

- Anisotropic volume conduction influences source strength and source orientation estimation more than source location estimation.
- Local conductivity properties in the vicinity of the source crucially influence source estimation.
- Model errors both on a local and a global scale are not Gaussian.